In vitro neurotoxicity hazard characterization of exhaust–derived particulate matter in rat primary cortical cultures using micro-electrode array recordings

Master Toxicology and Environmental Health
Major Research Project

Dirk C.A. de Leijer[1]
Under supervision of Lora-Sophie Gerber[1,2], Flemming R. Cassee[1,2], Remco H.S. Westerink[1]
[1]*Neurotoxicology Research Group, Toxicology Division, Institute for Risk Assessment Sciences (IRAS), Faculty of Veterinary Medicine, Utrecht University, Utrecht, The Netherlands*
[2]*Centre for Sustainability, Environment and Health, National Institute for Public Health and the Environment, Bilthoven, The Netherlands*

Abstract

Exposure to air pollution and particulate matter (PM) is linked to adverse health effects, including neurodegenerative diseases. While underlying mechanisms are still unknown, epidemiological studies have shown a strong correlation of these diseases with ultrafine particles (< 100 nm; UFP), which are mainly derived from traffic-related air pollution. Due to the small size, UFP can translocate to the brain through the cardiovascular system or directly enter the brain through the olfactory route and may negatively affect the central nervous system. The size distribution and chemical composition of traffic-related UFP can vary substantially between different types of engines and fuels, which in return potentially alters the neurotoxic potency of emitted PM. Aiming to shed light on the impact that different types of engine and fuel as well as UFP fractions have on the neurotoxic potency of traffic-related UFP, we screened several diesel exhaust-derived UFP and PM for their neurotoxic hazard.

UFP test samples where generated by light and heavy duty diesel engines fueled with high- or low-aromatic diesel and the non-volatile and semi-volatile UFP fractions were collected on Teflon filters. UFP samples were extracted and used for further neurotoxicity screening in rat primary cortical cell cultures grown on multi-well microelectrode arrays (MEA). To do so, spontaneous neuronal network activity was determined before and up to 120 h during UFP exposure (1-100 µg/mL and 1-20 L/mL). Additionally, cell viability was assessed after the final MEA recording to distinguish between specific neurotoxic effects and general cytotoxicity.

Exposure to diesel and biodiesel exhaust-derived PM decreased neuronal activity dose-dependent without affecting cell viability. However, diesel exhaust-derived PM was evidently more potent. Semi-volatile organic compounds (SVOC) UFP originating from high-aromatic (A20) and low-aromatic (A0) diesel fuel decreased the neuronal activity, although higher doses also exhibiting cytotoxicity. Interestingly, the non-volatile UFP fraction of A0 and A20 diesel fuel did not affect neuronal activity and cytotoxicity, indicating that the SVOC exhibited considerably higher neurotoxic potency than non-volatile UFP.

In the presented work, we demonstrated that diesel engine exhaust-derived UFP exhibit neurotoxic hazard, but also that the potency is dependent on sample generation conditions. Concluding, our data suggest that more emphasis should be placed on the emission of the SVOC fraction, which represent a larger hazard for brain health compared to the non-volatile fraction.

Layman summary

Coming in contact with traffic is inescapable, specifically in the many urban areas our world has to offer. In the car to work, on the sidewalk to the store and on the bicycle across town, people breathe in air polluted with traffic exhaust every day. This exhaust consists of many components, including particulate matter (PM). PM consist of mostly solid particles, with chemicals attached to them. They can be harmful to your lungs and enter the bloodstream from there. Moreover, the smallest particles, called ultrafine particles (UFP), can enter the brain directly via translocation the olfactory epithelial which is also know as the window into the brain. Therefore, it is important to investigate whether engine exhaust-derived UFP adversely affect the brain and its function. If so, it is also important to investigate which UFP exhibit the highest hazard and need to be reduced in our environment. With this aim in mind, we examined different sorts of UFP and their effect on brain activity of rat brain cells grown on a machine called the microelectrode array (MEA). These cells develop spontaneous activity over time which can be measured as electrical activity outside of the cells by the microelectrodes. The activity was recorded during exposure up to 5 days and compared to the activity before exposure to identify any differences in activity caused by the different samples. Decreasing the brain activity would mean that somewere in these brains cells, the particles disrupt a process and cause harm to the brain. We investigated the difference between the exhaust particles from diesel and biodiesel fuel and differences within fuel itself, among others. From this, we concluded that both diesel and biodiesel exhaust particles lowered brain activity, but that biodiesel was less harmful. Moreover, the fraction of the exhaust that is thought to be more harmful in general, the semivotalic organic compounds, also decreased brain activity more than other fractions. Therefore, we concluded that more attention should be paid to the use of biodiesel and lowering the semivotalic organic compounds in engine exhaust to reduce the risk on brain damage and human health overall.

TABLE OF CONTENTS

Introduction

Air pollution is recognized for its impact on human health. The World Health Organization (WHO) stated that 9 out of 10 people breath air that does not meet WHO air quality guidelines (WHO, 2016). Epidemiological studies indicate that airborne particulate matter (PM) is a pollutant within the ambient air pollution mixture that could be of specific importance related to human health (J. Chen & Hoek, 2020; Hamra et al., 2014; Hoek et al., 2013). According to an other WHO report , there is no evidence of a safe level of exposure for PM, which means that even the slightest quantity of PM can be hazardous for humans (WHO, 2013). In the analysis of the Global Burden of Disease study, ambient air PM pollution ranked fifth as an avoidable cause of death and sixth as a contributor to disability-adjusted life years lost (Cohen et al., 2017).

PM is usually classified in three categories by its aerodynamic diameter. Coarse particles less than than 10 µm in diameter are classified as PM10, fine particles less than 2.5 µm in diameter are classified as PM2.5 and the ultrafine particles (UFP), with a diameter less than 0.1µm are classified as PM0.1. The different fractions within air pollution are generally associated with a different origin, as coarse particles are mostly associated with mechanical processes as the generation of dust, whereas PM2.5 and UFP are more associated with physiochemical processes as combustion and gas to particle conversion (Manigrasso et al., 2020). Due to the small size, UFP have a considerably larger surface area relative to their mass than PM10 and PM2.5 (Kwon et al., 2020). With this larger surface area, more potentially toxic constituents, like chemicals, metals, endotoxins, can be attached to the particles present in the UFP mixture. While the underlying mode of action is not fully understood yet, exposure to UFP is known to induce inflammation, oxidative stress, and DNA damage (Bräuner et al., 2007; Kwon et al., 2020).

Many well-studied adverse effects of air pollution are known and encountered throughout the world, including cardiovascular (Lelieveld et al., 2019; Mannucci et al., 2019; Tibuakuu et al., 2018) and respiratory disease (Khreis et al., 2019; Kim et al., 2018; Zhu et al., 2019). Additionally, in recent years, evidence has been accumulating that air pollution may negatively affect the central nervous system (CNS) and contribute to neurodegenerative diseases, such as Parkinson's Disease (PD) and Alzheimer's Disease (AD) (Alemany et al., 2021; Block & Calderón-Garcidueñas, 2009; Calderón-Garcidueñas et al., 2021; H. Chen et al., 2017; Shi et al., 2021; Shin et al., 2018). Oxidative stress and neuroinflammation are thought to be the primary mechanisms of air pollution-induced neurotoxicity. Importantly, those mechanism are considered to be involved in the onset and progression of various neurodegenerative diseases (Genc et al., 2012; Gerlofs-Nijland et al., 2010; Levesque et al., 2011). In an *in vivo* study conducted by Campbell et al. (2004), mice were exposed to concentrated urban ambient air, filtered to contain only PM2.5 and UFP (4 h, 5 days per week for 2 weeks). The levels of proinflammatory cytokines IL-1α and TNF-α and immune-related transcription factor NF-κB in brain tissue were increased in mice exposed to PM as opposed to clean air, indicating a proinflammatory response in nervous tissue. Fagundes et al. (2015) exposed various rat brain cell tissues *in vitro* to PM2.5, collected by filtering urban ambient air. Hereafter, they evaluated oxidative stress parameters as the increase of lipid peroxidation and decrease of the antioxidant enzyme catalase for their involvement in neurotoxicity, concluding that PM induces oxidative stress and thereby damaging the brain.

For PM, the European Union (EU) has set Air Quality Standards for the limit values of total PM (PM10 and PM2.5 combined), PM10 and PM2.5 measured in ambient air that are monitored throughout the EU and legally binding for al EU Member States (European Parliament, 2008). In contrast, the monitoring and limit values of UFP lack, as studies on the adverse health effects of UFP are deemed inconclusive (European Parliament et al., 2021). However, the UFP fraction possibly exerts the most harm (Oberdörster et al., 2005; Traboulsi et al., 2017). Smaller particles are not cleared by broncho-mucociliary action or scavengered by alveolar macrophages. Particles in the UFP-size range can penetrate deep into the respiratory tract, up to the alveoli, where they can translocate into the bloodstream and from there, reach secondary target organs including the brain. This exposure route is known as the indirect, systemic route. Furthermore, metal-based nanoparticles falling in the UFP size range are also known to translocate directly through the olfactory mucosa into the olfactory bulb in vivo in various animal studies(Elder et al., 2006; Kanayama et al., 2005). Therefore, showing the possibility that UFP are transported through the direct, olfactory route into the brain, circumventing protective barriers as the blood-brain barrier.

Traffic is a major contributor to ambient air pollution and the associated PM (Ghio et al., 2012). Furthermore, diesel exhaust is seen as one of its most important components. Additionally, diesel is the fuel type for both, light- and heavy duty vehicles, as well as industrial machinery, diesel exhaust-derived PM exposure (Costa et al., 2017). Therefore, it is often utilized as a measure of traffic-related air pollution. Diesel exhaust, produced and released during the combustion of diesel fuel, is a complex mixture of gases (e.g. nitrogen oxides and carbon monoxide), hydrocarbons (e.g. aldehydes, volatile organic compounds and polycyclic aromatic hydrocarbons) and particles (e.g. organic and elemental carbon) (Hesterberg et al., 2011). To date, the polycyclic aromatic hydrocarbons (PAH), a subgroup of the semivolatile organic compounds (SVOC) and metals are the UFP that are thought to be the most harmful within diesel exhaust-derived PM. While metals occur naturally in fossil fuels (de Kok et al., 2006), aromatics compounds are added to the fuel as engine lubricant oils and account for 10-30% of regular diesel fuel (Qian et al., 2017). Because of incomplete combustion of the fuel, they are transformed to SVOC in the exhaust (L. Huang et al., 2013). Both PAHs and metals are presumed to contribute to the induction of oxidative stress, cytoxicity and mutagenicity from traffic exhaust exposure, and are thought to be more abundant in the smaller PM2.5 and UFP fractions as opposed to the total suspended particles and PM10 (de Kok et al., 2006).

Therefore, the generation conditions of different UFP are important to assess the potential neurotoxicological hazard of engine exhaust-derived PM. Differences in fuel types, engine types and exhaust fractions could lead to an entirely different composition of the samples. For instance, the difference between petroleum-derived diesel fuel (regarded as regular diesel), and biodiesels blends generate different PM mass and concentrations (McCormick et al., 2006). Biodiesel is made from renewable sources and therefore, it is seen as a 'greener' option than regular diesel from fossil fuel sources. Generally, biodiesel is a fuel-blending component produced from vegetable oils, animal fats, or waste grease and is typically blended with fossil diesel up to 20%.

In this study, the effects of various fuel types, engine types and exhaust fractions were assessed, with specific emphasis on their potential hazard characterization. The various samples included in this study were diesel and biodiesel exhaust-derived PM2.5, the diesel exhaust-

derived UFP from an older EURO 2-compliant and a newer EURO 6-compliant engine and the non-volatile UFP and SVOC UFP fractions of a low aromatic (A0) and high aromatic (A20) engine fuel (further abbreviated to non-volatile A0 and A20, and SVOC A0 and A20). Additionally, carbon and copper oxide nanoparticles serving as a benchmark material were included. With this approach, this study investigated the potential neurotoxic hazards of several engine and fuel types. To do so, the neuronal network activity of rat primary cortical cultures was examined on different timepoints after exposure to the different samples with the use of the multi-well Micro-Electrode Array (MEA) recordings. The MEA is a non-invasive technique that was capable of detecting changes in spontaneous neuronal (network) activity by a raster of micro electrodes within each well. These microelectrodes measured the extracellular field potentials and transformed them to parameters characterizing the neuronal (network) activity, e.g. the number of spikes, bursts and network bursts (fig. 1) (Gerber et al., 2021).
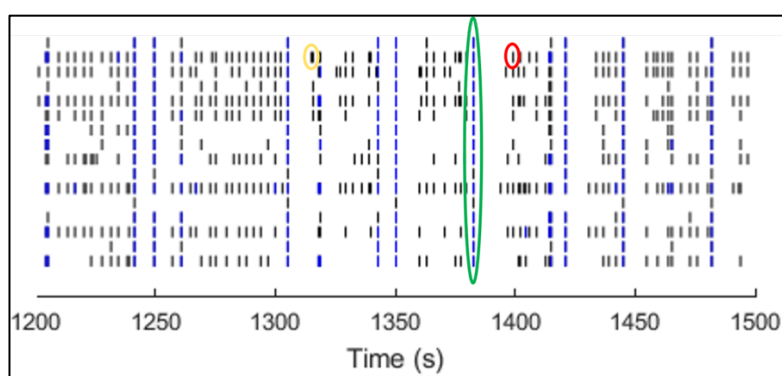

Figure 1: Raster plot of neuronal activity of primary rat cortical cultures on the MEA in the timeframe of 1200-1500 seconds. Baseline recording (DIV9) including spikes (shown in yellow), bursts (red) and network bursts (green). Spikes represent the extracellular field recordings of action potentials, bursts represent a series of spikes within a short interval recorded by a single electrode, and network bursts represent the combination of bursts over multiple electrodes within a short interval within a single well.

Recently, the technique has been used in studies on neurotoxicity testing of chemicals, toxicants and (illicit) drugs (Hondebrink et al., 2016; Vassallo et al., 2017; Zwartsen et al., 2018) but it was demonstrated that MEA recordings are also applicable to assess the neurotoxicity of metal-based nanoparticles (Strickland et al., 2015). Using the MEA as a method to investigate the effects on neuronal (network) activity integrated the underlying mechanisms that can affect the activity, including cell viability, network integrity, synaptic transmission, ion channel and receptor functions. Whereas most studies *in vitro* on the neurological effect of PM focus mostly on single endpoints, the MEA allowed us to study the neurotoxicity of the samples and rank them on their potential hazard in a more integrated approach.

Rat primary cortical cultures possess many characteristics closely related to the human brain, as they form neuronal networks and develop spontaneous network activity (Charlesworth et al., 2015; Chiappalone et al., 2007). They primarily consist of astrocytes and neurons, including excitatory glutamergic and inhibitory GABAergic neurons (Hondebrink et al., 2016). Postnatal rat primary cortical cultures were exposed on Day In Vitro (DIV) 9 and MEA recordings were performed directly before and after exposure, as well as after 24 h, 48 h and 120 h after exposure in different doses to investigate the effect of the samples on neuronal (network) activity in a concentration- and time-dependent manner acutely and subchronic (Gerber et al., 2021). The neurotoxic effect of traffic-derived PM *in vivo* and to a lesser extend *in vitro* was studied, but the

combination with the MEA and the neuronal (network) activity of primary rat cortical cultures to investigate the effect of UFP has helped us to understand the potential neurotoxicity of traffic-derived UFP.

Materials & methods

Chemicals

Neurobasal-A (NBA) media, L-glutamine (200 mM), Penicillin/Streptomycin (5000 U/mL/5000 mg/mL), and B-27 Plus Supplement (50X) were obtained from Thermo Fisher Scientific (Bleiswijk, The Netherlands). All other chemicals were purchased from Sigma-Aldrich (Zwijndrecht, The Netherlands). The test samples were provided by the National Institute for Public Health and the Environment (Rijkinstituut voor Volkgezondheid en Milieu; RIVM) and the University of Eastern Finland (UEF).

Test samples and reconstruction

In table 1, information about the test samples, including reference materials, collected exhaust fraction, fuel or engine types used to generate the sample, providers, collected/primary size ranges and tested concentration ranges, was summarized.

Table 1: Overview of the tested samples. PM, particulate matter; SVOC, semivolatile organic compounds; RIVM, National Institute for Public Health and the Environment; UEF, University of Eastern Finland

Sample ID	Sample or fuel type	Engine type	Provider	Collected/ primary size range	Conc. range
Blank extract	Clean air filter extract	-	UEF	-	1 – 100 µg/mL
Carbon particles	Carbon electrode	VSP generator	UEF	PM0.1	1 – 100 µg/mL
Copper oxide particles	Purchased from PlasmaChem*	-	RIVM	PM0.1	0.1 – 1 µg/mL
Diesel	EN590 diesel	Common rail engine diesel generator	RIVM	PM2.5	1 – 100 µg/mL
Biodiesel	EN590 diesel + 20% biofuel	Common rail engine diesel generator	RIVM	PM2.5	1 – 100 µg/mL
EURO 2 engine	EN590 diesel	Non-road Kubota engine (EURO 2)	UEF	PM0.1	1 – 100 µg/mL
EURO 6 engine	EN590 diesel	Skoda Octavia diesel engine (EURO 6)	UEF	PM0.1	1 – 100 µg/mL
Non-volatile A0	Low aromatic diesel	heavy duty diesel engine (AGCO)	UEF	PM0.1	1 – 100 µg/mL
Non-volatile A20	High aromatic diesel	heavy duty diesel engine (AGCO)	UEF	PM0.1	1 – 100 µg/mL
SVOC A0	Low aromatic diesel	heavy duty diesel engine (AGCO)	UEF	PM0.1	1 – 20 L/mL
SVOC A20	High aromatic diesel	heavy duty diesel engine (AGCO)	UEF	PM0.1	1 – 20 L/mL

* Germany, Cat. PL-CuO, Lot. YF131107

All solid particles samples provided in glass vials by UEF (Carbon particles, EURO 2 engine, EURO 6 engine, non-volatile A0 and A20) were dispersed in 100% DMSO to a 100 mg/mL concentration. Since test samples were attached to the glass of the vial, a sterile glass rod was used to scrape off the sample. Further, samples were vortexed to get the solid particles in dispersion. Glutamate-free culture medium, containing Neurobasal-A (NBA) medium, supplemented with 25 g/L sucrose, 450 µM L-glutamine, 1% penicillin/streptomycin and 10% FBS, pH was set to 7.4, was added to reach a stock concentration of 5 mg/mL containing 5% v/v DMSO. After sonication (10 minutes in a ultra sonic bath), exposure solutions with a concentration range of 10 – 1.000 µg/mL with a 1% v/v DMSO content were obtained by further diluting the stock solution with glutamate-free culture medium. For glass vials containing 0.5 mg sample, the DMSO and glutamate-free culture media volumes were adjusted, and two separate glass vials were combined.

The blank extract provided by UEF is collected by running fresh air through the system using the same collection process as for the solid particles samples from UEF to assess whether the extraction process could affects neuronal activity or cell viability. Since no mass is collected on the filter from fresh air, the corresponding volume of the solid particles samples was used as a reference for the collected volume. This conversion was used to express the further experiment in the doses equal to those of the solid particles samples.

Copper oxide particles provided by RIVM were reconstructed in ddH_2O to a concentration of 100 mg/mL, sonicated (10 min; ultra sonic bath), and further diluted with glutamate-free culture medium to get exposure solutions with a concentration range of 0.1 – 10 μg/mL with a 1% v/v ddH_2O content.

Diesel and Biodiesel exhaust-derived PM samples provided by RIVM were reconstructed in 100% DMSO to a stock concentration of 100 mg/mL, vortexed, and used for exposure directly or stored at -20°C for further experiments. Before exposure, the stock samples were sonicated (10 min; ultra sonic bath) and further diluted with glutamate-free culture medium to prepare exposure solutions. As with the solid particles samples from UEF, a concentration range of 10 – 1.000 μg/mL containing 1% DMSO was prepared and used for exposure.

The SVOC samples were reconstructed in glutamate-free culture media containing 5% v/v DMSO to a concentration of 1000 L/mL. Following sonication (10 min; ultra sonic bath), exposure solutions were prepared by further diluting the stock with glutamate-free culture media to a concentration range of 10 – 200 L/mL with a 1% v/v DMSO content.

Cell cultures

Animal experiments were performed in agreement with Dutch law, the European Community directives regulating animal research (2010/63/EU), and approved by the Ethical Committee for Animal Experiments of Utrecht University. All efforts were made to minimize the number of animals used and their suffering.

Rat primary cortical cultures were prepared from Wistar rat pups (Envigo, Horst, the Netherlands) and cultured as described previously by Gerber *et al.* (2021). Briefly, cells were isolated and 10^5 cells were seeded on 0.1% polyethyleneimine (PEI)-coated 48-wells MEA-plates (Axion Biosystems Inc., Atlanta, GA, USA) in 50 μL dissection medium containing Neurobasal-A (NBA) medium, supplemented with 25 g/L sucrose, 450 μM L-glutamine, 30 μM glutamate, 1% penicillin/streptomycin and 10% FBS and the pH was set to 7.4. Afterwards, cells were allowed to attach to the electrode grid by incubating at 37°C, 5% CO_2, and 95% air atmosphere for 2h before 450 μL of dissection media was added to each well.

On day *in vitro* (DIV) 4, 90% of the dissection media was replaced by glutamate-free culture medium. On DIV 8, one day before the MEA recording experiment started and cells were exposed, 50% of the glutamate-free culture medium was replaced. To account for evaporation over time, 5 μL and 20 μL sterile ultra-pure water was added to the inner and outer wells, respectively, before medium change.

MEA recording experiments

MEA recording experiments started on DIV 9 when rat primary cortical cultures exhibit stable spontaneous neuronal activity (Dingemans et al., 2016). To investigate the effects of the samples on spontaneous neuronal (network) activity, MEA recordings were performed directly after exposure (0.5 h exposure), and after subchronic exposure on DIV 10, DIV 11, and DIV 14 (24 h, 48 h, and 120 h exposure, respectively).

Each well of an MEA plate contains an electrode array of 16 nanotextured gold micro-electrodes (40–50 μm diameter; 350 μm center-to-center spacing) which are recorded at the same time (Tukker et al., 2018). The Maestro 768-channel amplifier was equipped with an integrated heating system, temperature controller, and a data acquisition interface (Axion Biosystems Inc., Atlanta, GA, USA). Data acquisition was managed with Axion's Integrated Studio (AxIS version 2.5.2). Signals were pre-amplified with a gain of 1200x (61 dB), band-pass filtered at 0.2–5 kHz, and sampled simultaneously resulting in raw (.RAW) data files.

Before exposure, baseline activity of the rat primary cortical culture was recorded for 30 min (baseline recording) after a calibration time of 5 minutes. Afterwards, cells were exposed by adding 55 μL of the freshly prepared exposure solutions to each well, which results in a 10x dilution. Therefore, all particulate matter (PM) samples reconstructed in DMSO have a final concentration of 1 – 100 μg/mL, and SVOC samples reconstructed in DMSO have a final concentration of 1 – 20 L/mL, with a 0.1% v/v DMSO content for both PM and SVOC. The copper oxide particles final concentration ranges from 0.01 – 1 μg/mL with a ddH_2O concentration of 0.1% v/v due to cytotoxicity at higher doses. For all samples, 0.1% v/v solvent (DMSO or ddH_2O, respectively) in glutamate-free culture medium was used as control. Remaining exposure solutions are frozen and kept at -20 ˚C for further size distribution analysis.

Directly after exposure, MEA recording comprising of 30 minutes after a calibration time of 5 minutes was conducted to assess acute effects. Further MEA recordings took place after 24 h, 48 h, and 120 h of exposure. Between the recordings, the cells were kept at 37˚C, 5% CO_2, and 95% air atmosphere. For the experiments, all conditions were tested on rat primary cortical cultures originating from at least 3 different isolations, in at least 3 plates (N) and at least 16 wells (n). The number of wells represents the number of replicates per condition.

Cell viability assay

On DIV 14, after the final MEA recording, an Alamar Blue Assay was performed to discriminate between specific neurotoxic and general cytotoxic effects. The Alamar Blue assay provides an indirect quantification of the cell viability by assessing the mitochondrial activity of cells using the blue, non-fluorescent resazurin which is reduced to the red, fluorescent resorufin by the mitochondrial product NADH. For the cell viability assay, a 25 μM Alamar Blue working solution was prepared by diluting the stock (5 mM resazurin in PBS) in HBSS. The medium of the wells was replaced by 300 μL of the Alamar Blue working solution and cells were incubated for 1.5 h at 37˚C with 5% CO_2 and 95% air atmosphere. Subsequently, of each well, 200 μL incubated Alamar Blue working solution was transferred to a transparent 96-wells plate. Additionally, 200 μL of the Alamar Blue working solution was added to four extra wells serving as a blank control. The fluorescence was measured using a microplate reader (Infinite M200, TECAN, Switzerland) with an excitation wavelength of 540 nm and an emission wavelength of 590 nm.

An Alamar Blue Assay was performed with carbon and copper oxide particles to account for possible interference from particles known to affect fluorescence (Breznan et al., 2015). Excess exposure solution from the MEA recording experiments was collected for three doses of both copper and carbon oxide particles. 20 µL per concentration was diluted with 180 µL of either fresh resazurin or the reduced resorufin to obtain final doses of 1, 10 and 30 µg/mL for carbon particles and 0.01, 0.1 and 1 µg/mL for copper oxide particles in resazurin and in resorufin. Additionally, 200 µL of resazurin and 200 µL of resorufin was added to three extra wells each as a control. The fluorescence was measured using a microplate reader (Infinite M200, TECAN, Switzerland) with an excitation wavelength of 540 nm and an emission wavelength of 590 nm.

Size distribution analysis

The particle size distribution (expressed as the hydrodynamic radius) of the samples was measured using Dynamic Light Scattering (DLS) (Zetasizer Ultra, Malvern Panalytical Ltd., Malvern, UK). Remaining exposure solution from the MEA experiments were thawed for 0.5 h at room temperature and sonicated for 10 minutes. To obtain identical doses as for the MEA recording experiments, the exposure solutions were 10x diluted with glutamate-free culture medium**.** For DLS measurements, the samples were vortexed and approximately 1 mL of the dilution was transferred to a polysterene cuvette. The optimal dispersant scattering mean count rate (kcps) and attenuation were assessed using glutamate-free culture medium and the ZS Explorer software (Version 1.0.0, Malvern) and set on 340 and 9 for the kcps and attenuation respectively. The equilibrium time was set on 30 seconds, as the samples are on room temperature. Afterwards, the DLS size distribution is measured one time, the particle concentration three times and the multi-angle DLS (MADLS) one time, in sequence with no equilibriation time in between. The median particle diameter (D50) of the highest doses was used as the representative value for the size of the particles.

Data Analysis

For the MEA recordings analysis, spike data were extracted from the MEA recordings raw files, as mentioned earlier. These raw data files were re-recorded, and spikes were detected using the AxIS spike detector (Adaptive threshold crossing, Ada BandFlt v2) with a post and pre spike duration of 3.6 2.4 ms, respectively, and a variable threshold spike detector set at 7x standard deviation (SD) of the internal noise level (rms) on each individual electrode to obtain spike files (.spk). The spike files were loaded into NeuralMetric Tool (version 3.1.7 Axion BioSystems) for further analysis. To do so, the last 10 minutes of each recording (baseline and exposure) were used for data analysis and subsequent settings were chosen: only active electrodes (MSR ≥ 6/minute) within active wells (≥ 1 active electrode) were included, also excluding coincident artifacts; The Poisson Surprise method (Legendy & Salcman, 1985) was used to detect the bursts and network bursts with a minimal surprise of 10 and with an Inter-Spike-interval (ISI) threshold algorithm with a minimum of 40 spikes, maximal ISI of 100 ms, and a minimum of 15% active electrodes, respectively. The now obtained Comma Separated Values (.csv) files were used to compute the treatment ratios for a set of neuronal activity parameters by custom-made MS Excel macros. The treatment ratios were calculated for each well and each parameter by dividing the exposure values by the corresponding baseline value (exposure/baseline). After outlier analysis in the control wells (≥2x SD; %, Table 2A), treatment ratios of the exposure wells were normalized to the treatment ratios of the control. Finally, the replicates of the experiments (N) were combined and outlier analysis was also performed for exposure wells (≥2x SD; %, Table 2B).

Table 2: Percentage of excluded outliers, relative to the total amount of wells for the control (A) and the exposure conditions (B). Expressed as the mean percentage of all exposure conditions.

A	0.5 h	24 h	48 h	120 h
MSR	1.8	2.1	1.7	2.9
MBR	3.0	2.3	3.4	4.3
MNBR	3.2	1.9	2.3	4.1

B	0.5 h	24 h	48 h	120 h
MSR	4.1	3.8	4.6	4.7
MBR	4.5	5.1	4.4	4.5
MNBR	4.7	5.0	4.6	5.1

For the cell viability assay analysis, the average of the blank was subtracted from raw values to correct for background fluorescence. Afterwards, the average of the control was calculated and values for exposure wells were normalized to control average (control set to 100% mitochondrial activity). Experiments were combined and averages of metabolic activity per concentration were calculated. Values exceeding 2x SD are considered to be outliers and excluded from the analysis. The values are normalized to control and expressed in the mean percentage of control, where the control is set to 100%.

For size distribution, measurements were analyzed using ZS Xplorer (Version 1.0.0, Malvern) and the D50 values of the hydrodynamic diameter were used to assess the median and standard deviation.

Statistical analysis

All statistical analyses were performed using GraphPad Prism (version 9.0.0, GraphPad Software, La Jolla CA, USA). Welch's ANOVA followed by a Dunnett's T3 multiple comparisons test were used to determine the significant changes in neuronal activity parameters of exposure compared to control. The resulting data is presented as mean ± standard error of the mean (SEM) normalized to the control. P-values < 0.05 were considered statistically significant. Significant effects on neuronal activity within 75-125 were considered to be of limited toxicological relevance. One-way ANOVA followed by *post-hoc* Dunnett's multiple comparisons test was used to determine significant changes in mitochondrial activity for the cytotoxicity analysis. The resulting data is presented as mean ± SD normalized to the control. P-values < 0.05 were considered statistically significant.

Results

Acute and subchronic exposure to the blank extract did not affect neuronal activity or viability

The blank control assessed differences potentially made by the extraction method. Therefore, no particles were collected and the doses mentioned are regarded as equivalent of the other sample doses. None of the tested doses of the blank extract did induce relevant change of MSR and MBR at any time point (0.5 h, 24 h, 48 h or 120 h; fig. 2A). MNBR was reduced after acute and 120 h exposure to a dose of 1 µg/mL and 30 µg/mL, respectively. However, no concentration- or time-dependent relationship was observed. Furthermore, 120 h exposure to the blank extract did not reduce the metabolic activity of the culture (fig. 2B). Therefore, we concluded that the blank filter extract did not exhibit relevant effects on neuronal (network) activity or viability of the rat primary cortical cultures and that in further experiments 0.1% DMSO can be used as control.
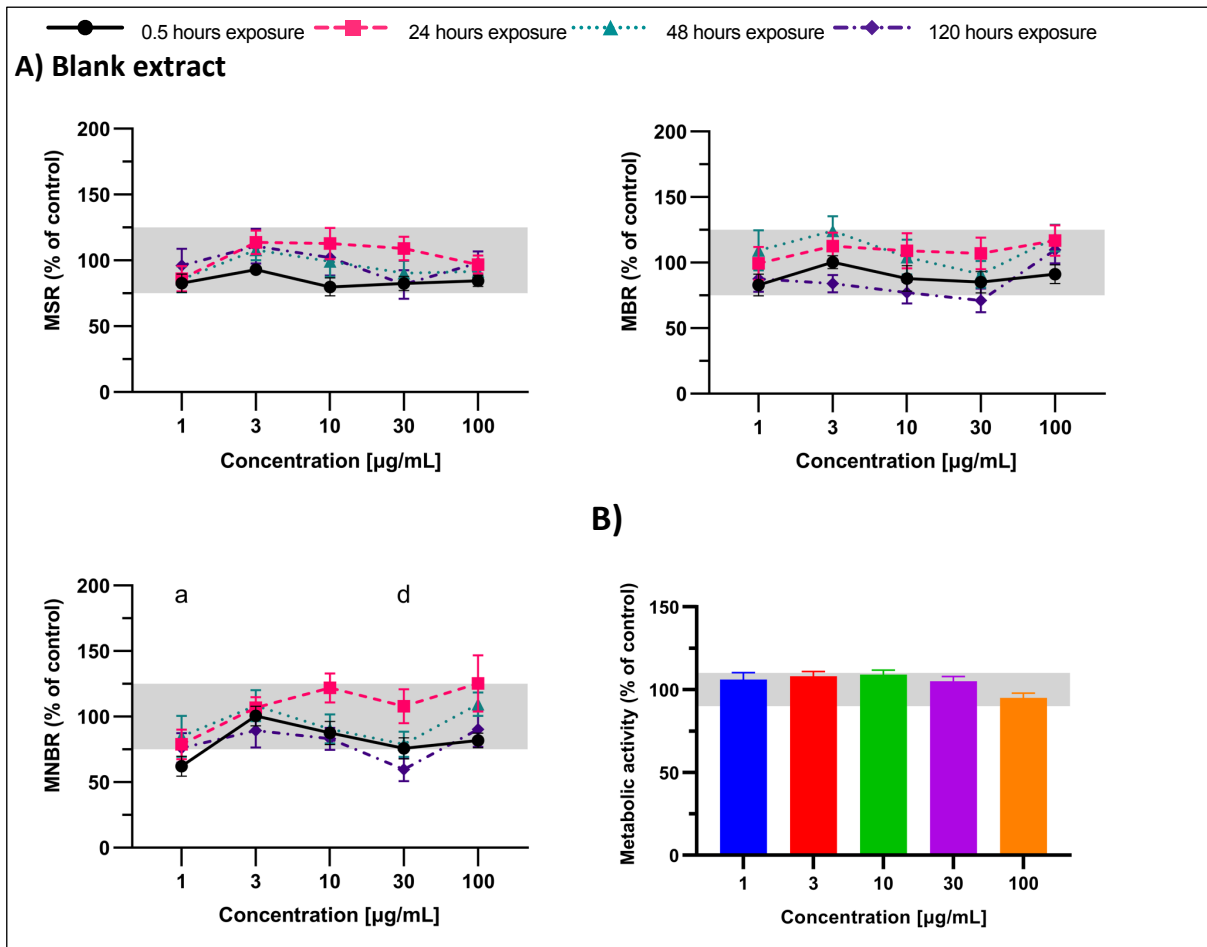
Figure 2: Effect of Blank extract on neuronal (network) activity (A) and metabolic activity (B) of rat primary cortical cultures. Effects on neuronal activity were assessed after 0.5 h, 24 h, 48 h and 120 h exposure. Mean Spike Rate (MSR), Mean Burst Rate (MBR), and Mean Network Burst Rate (MNBR) are presented as mean treatment ratio (± SEM) normalized to control from n = 18 - 24 wells, N = 3. Effects ≤ 25% (2xSD of control; indicated by the grey area) are considered to be of limited toxicological relevance. Significant effects were determined by Welch's ANOVA and if exceeding 25% of control indicated by [a]=p < 0.05 for 0.5 h exposure compared to time-matched control, [b]=p < 0.05 for 24 h exposure compared to time-matched control, [c]=p < 0.05 for 48 h exposure compared to time-matched control, [d]=p < 0.05 for 120 h exposure compared to time-matched control. Cell viability was determined after 120 h exposure and data is presented as mean (± SD) normalized to control from n = 19 - 24 wells, N = 3. Effects ≤ 10% (indicated by the grey area) are considered as biological variability. Significant effects were determined by ordinary one-way ANOVA. *=p < 0.05 compared to control and exceeding 10%.

Carbon and Copper oxide particles exposure did not induce change in neuronal activity in non-cytotoxic range

For acute and subchronic exposure to 1 - 100 µg/mL carbon particles no change in any of the neuronal activity parameters was observed (fig. 3A). However, after 120 h exposure the metabolic activity was significantly decreased at 30 µg/mL (fig. 4A), indicating decreased cell viability.

Copper oxide particles decreased the MSR, MBR and MNBR after subchronic 24 h exposure to 1 µg/mL (fig. 3B). However, after 120 h the metabolic activity shows a concentration-dependent reduction for concentration from 0.3 µg/mL (fig. 4B).
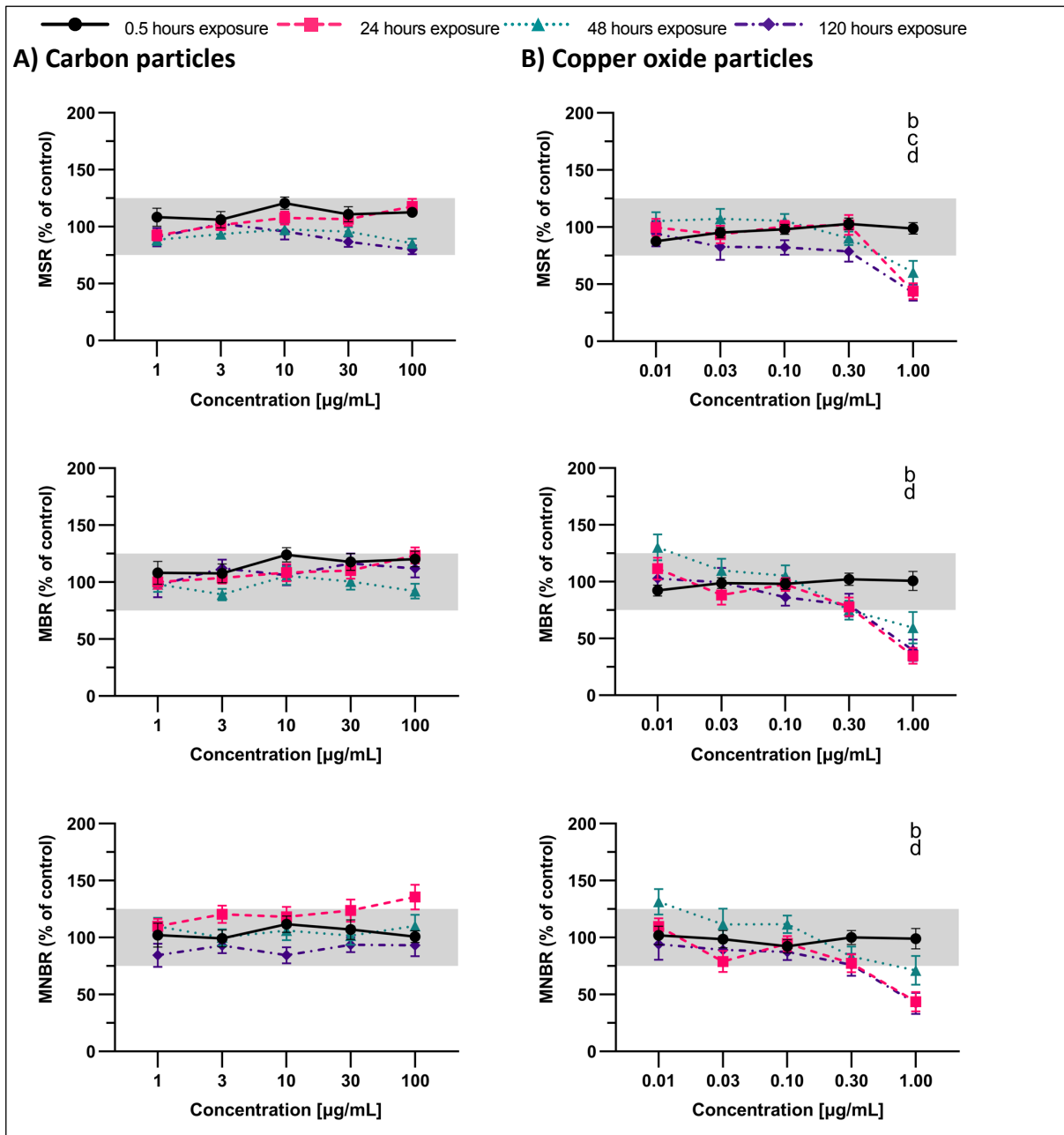
Figure 3: Effect of Carbon particles (A) and Copper oxide particles (B) on neuronal (network) activity of rat primary cortical cultures. Effects on neuronal activity were assessed after 0.5 h, 24 h, 48 h and 120 h exposure. Mean Spike Rate (MSR), Mean Burst Rate (MBR), and Mean Network Burst Rate (MNBR) are presented as mean treatment ratio (± SEM) normalized to control from n = 18 - 24 wells, N = 3. Effects ≤ 25% (2xSD of control; indicated by the grey area) are considered to be of limited toxicological relevance. Significant effects were determined by Welch's ANOVA and if exceeding 25% of control indicated by [a]=p < 0.05 for 0.5 h exposure compared to time-matched control, [b]=p < 0.05 for 24 h exposure compared to time-matched control, [c]=p < 0.05 for 48 h exposure compared to time-matched control, [d]=p < 0.05 for 120 h exposure compared to time-matched control.
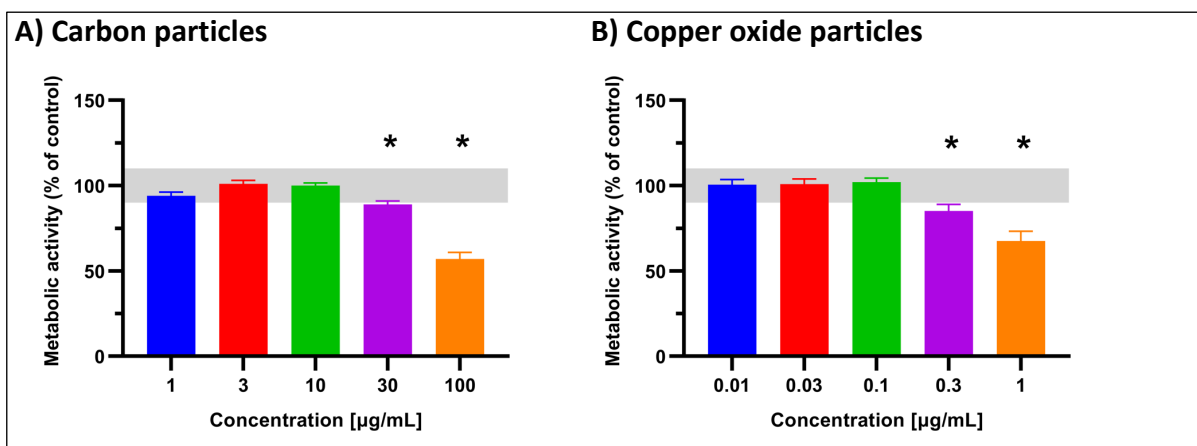
Figure 4: Effect of Carbon particles (A) and Copper oxide particles (B) on metabolic activity of rat primary cortical cultures after 120 h exposure. Cell viability data is presented as mean (± SD) normalized to control from n = 19 - 24 wells, N = 3. Effects ≤ 10% are of limited toxicological relevance and indicated by the grey area. Significant effects were determined by ordinary one-way ANOVA. *=p < 0.05 compared to control and exceeding 10%.

To investigate the possible interference of carbon and/or copper oxide particles, three doses of each sample group were diluted with either resazurin or resorufin and fluorescence intensity was measured (fig. 5). Carbon particles show a signicant difference from the control for 30 mg/mL for both resazurin and resorufin, the same concentration that shows an significant decrease for the Alamar Blue assay (fig. 4A). Copper oxide particles do not show a significant decrease for both resazurin and resorufin, indicating no interference for the Alamar Blue assay (fig. 4B)
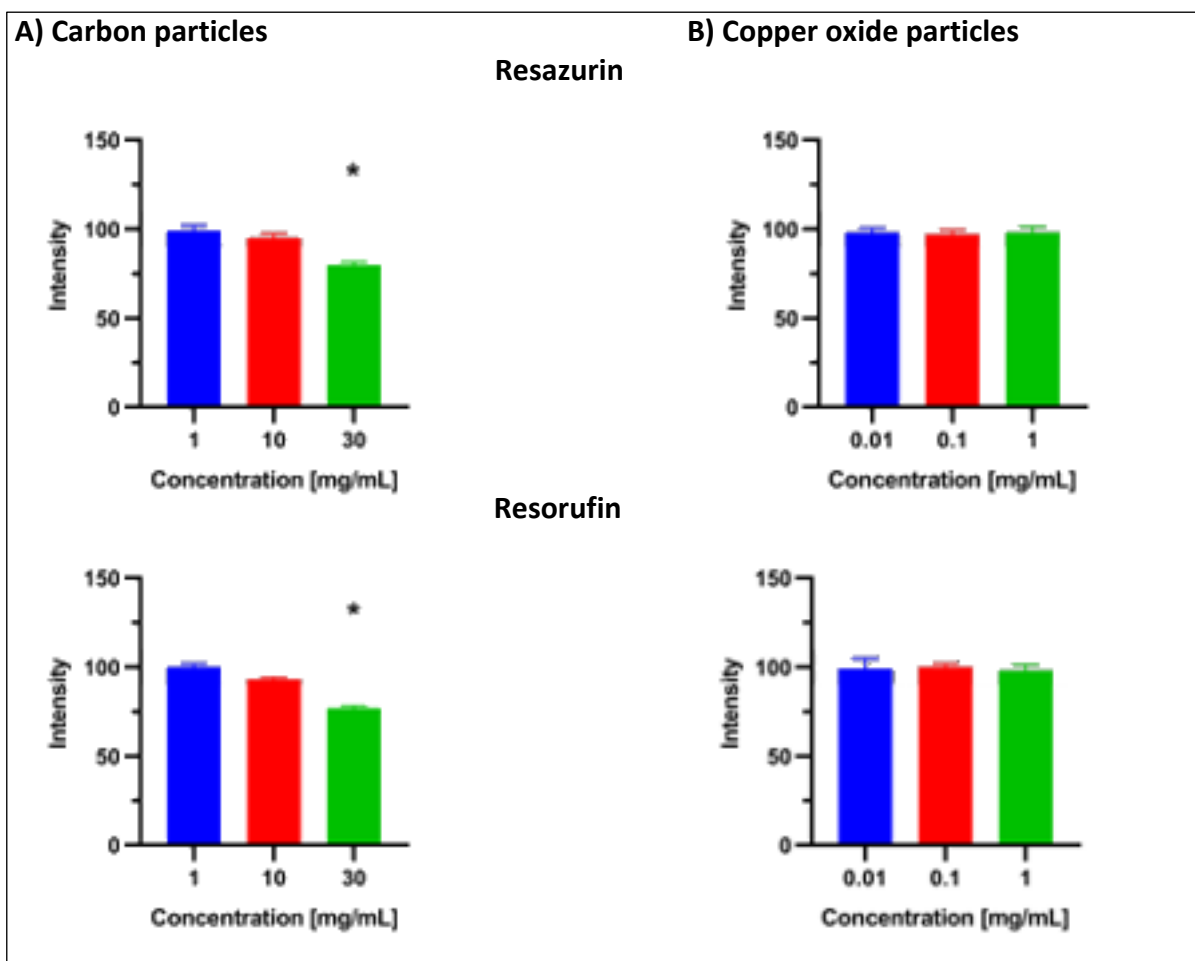
Figure 5: Effect of Carbon particles (A) and Copper oxide particles (B) on fluorescence intensity after 120 h exposure. Top and bottom row show the combination with resazurin and resorufin respecvtively. Fluorescentce intensity data is presented as mean (± SD) normalized to control from n = 3 wells, N = 1. Significant effects were determined by ordinary one-way ANOVA. *=p < 0.05 compared to control.

Diesel and Biodiesel exhaust-derived PM reduce neuronal activity

For acute exposure, only the highest concentration of 100 µg/mL diesel exhaust-derived PM reduced the MBR (fig. 6A) to 61.9% (p = <0.0001). Following subchronic exposure (24 h, 48 h and 120 h), MSR, MBR and MNBR were significantly and dose-dependently decreased by 30 µg/mL. Furthermore, 120 h exposure to 10 µg/mL diesel exhaust-derived PM significantly reduced the MBR to 69.1% (p = 0.0063). For the biodiesel exhaust-derived PM no effect was seen after acute exposure. After 24 h exposure to 100 µg/mL a mild reduction of MSR, MBR and MNBR was observed while MNBR was not reduced significantly after 120 h to 100 µg/mL (fig. 6B). Both, diesel or biodiesel exhaust derived PM did not induce change in metabolic activity after 120 h indicating that cell viability was unaffected (fig. 7).
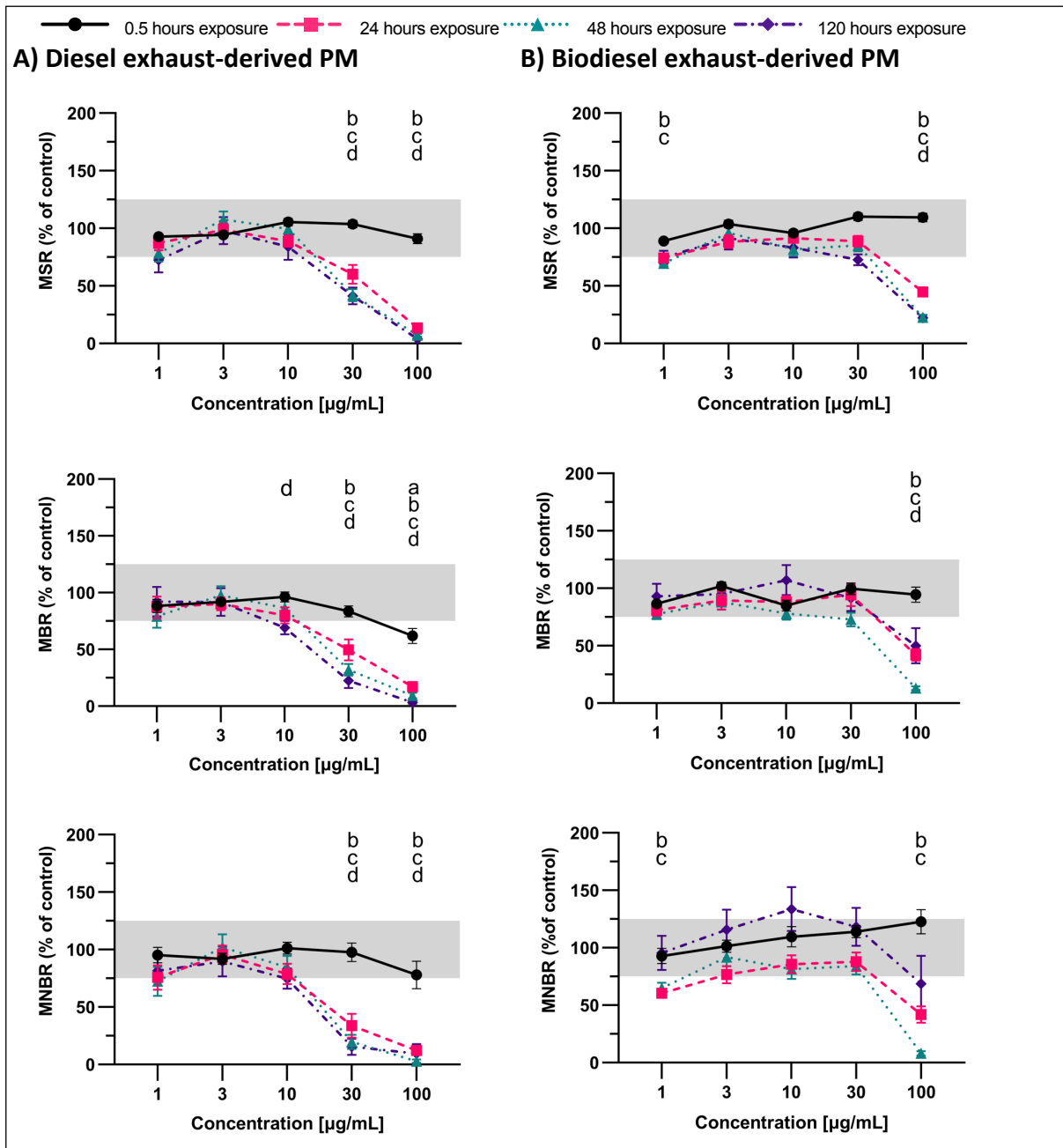
14

Figure 6: Effect of Diesel exhaust-derived PM (A) and Biodiesel exhaust-derived PM (B) on neuronal (network) activity of rat primary cortical cultures. Effects on neuronal activity were assessed after 0.5 h, 24 h, 48 h and 120 h exposure. Mean Spike Rate (MSR), Mean Burst Rate (MBR), and Mean Network Burst Rate (MNBR) are presented as mean treatment ratio (± SEM) normalized to control from n = 18 - 24 wells, N = 3. Effects ≤ 25% (2xSD of control; indicated by the grey area) are considered to be of limited toxicological relevance. Significant effects were determined by Welch's ANOVA and if exceeding 25% of control indicated by [a]=p < 0.05 for 0.5 h exposure compared to time-matched control, [b]=p < 0.05 for 24 h exposure compared to time-matched control, [c]=p < 0.05 for 48 h exposure compared to time-matched control, [d]=p < 0.05 for 120 h exposure compared to time-matched control.
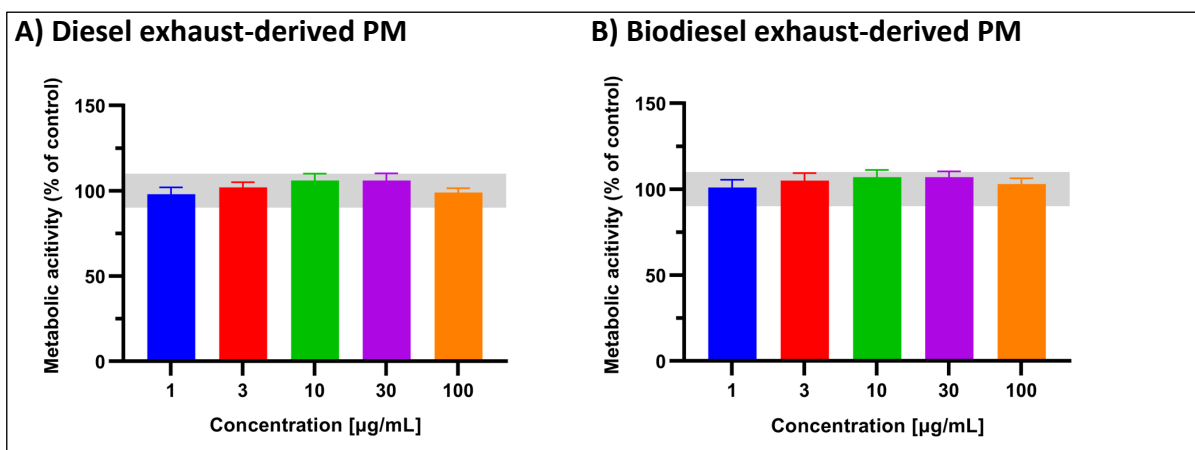
Figure 7: Effect of Diesel exhaust-derived PM (A) and Biodiesel exhaust-derived PM (B) on metabolic activity of rat primary cortical cultures after 120 h exposure. Cell viability data is presented as mean (± SD) normalized to control from n = 19 - 24 wells, N = 3. Effects ≤ 10% are of limited toxicological relevance and indicated by the grey area. Significant effects were determined by ordinary one-way ANOVA. *=p < 0.05 compared to control and exceeding 10%.

EURO 2 engine exhaust-derived PM reduces neuronal activity, while EURO 6 engine exhaust-derived PM did not

EURO 2 engine exhaust-derived PM decreased the MSR and MBR after 48 h exposure to 100 µg/mL and to 30 µg/mL for the MNBR to 69.3% (p = 0.0003), 70.8% (p = 0.0044) and 62.0% (p = 0.007) respectively (fig. 8A). Furthermore, an increase of activity for the MBR after 120 h exposure to 1 and 3 µg/mL is shown. As the 120 h exposure values show a relatively large SEM and an inconsistent trend, the significant increase for 1 and 3 µg/mL after 120 h exposure is considered an artefact and of limited toxicological relevance. Cell viability after 120 h exposure to 100 µg/mL is minorly but significant decreased to 87.0% (p = 0.0003) (fig. 9A). EURO 6 engine exhaust-derived PM decreased the MNBR after 120 h exposure to 30 µg/mL slightly to 74.8% (p = 0.0426) (fig. 8B). For the other parameters, no effects were observed. Similarly, cells exposed to EURO 6 engine exhaust-derived PM for 120 h exhibit same viability as control cells (fig. 9B).
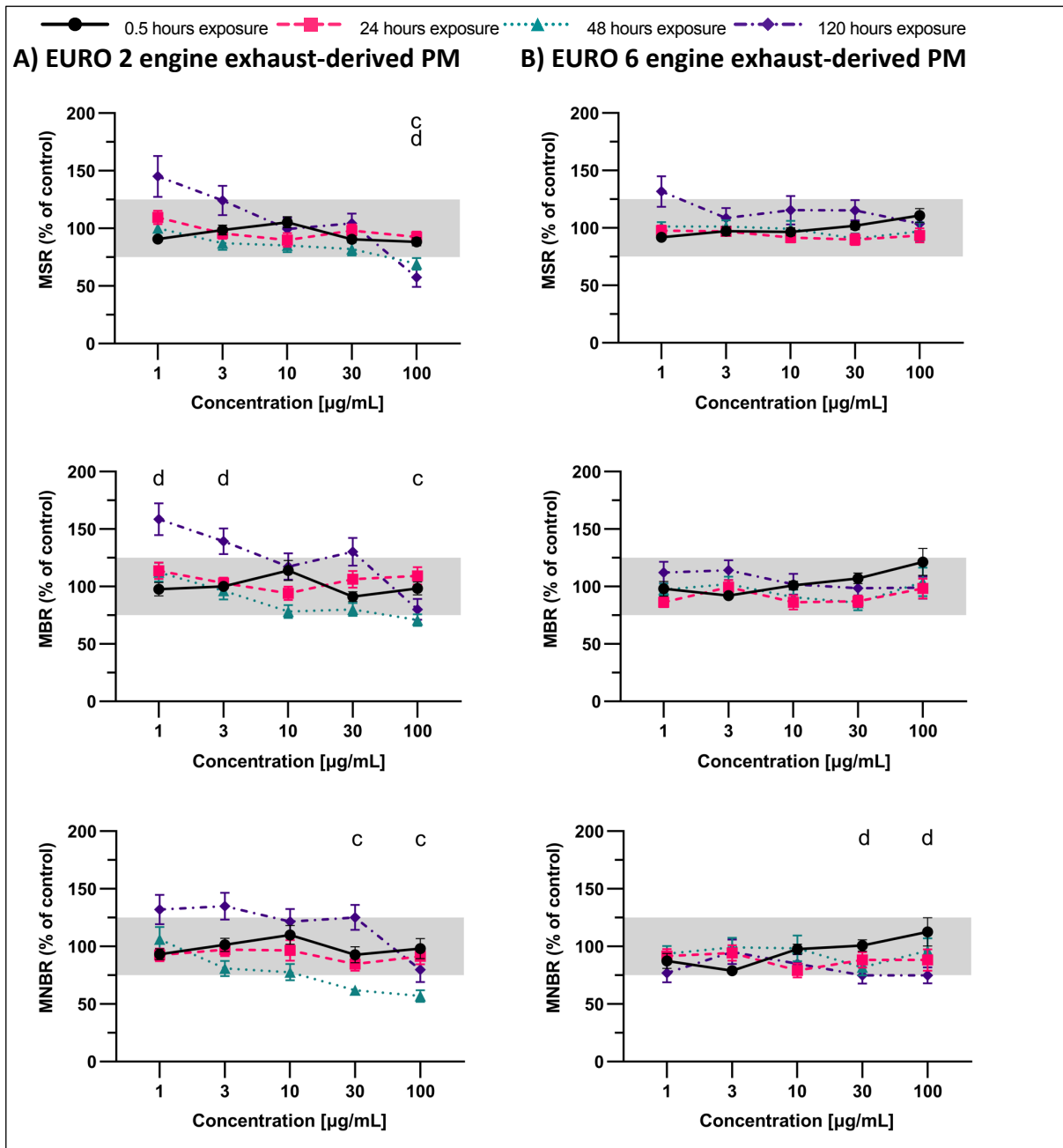
16

Figure 8: Effect of EURO 2 engine exhaust-derived PM (A) and EURO 6 engine exhaust-derived PM (B) on neuronal (network) activity of rat primary cortical cultures. Effects on neuronal activity were assessed after 0.5 h, 24 h, 48 h and 120 h exposure. Mean Spike Rate (MSR), Mean Burst Rate (MBR), and Mean Network Burst Rate (MNBR) are presented as mean treatment ratio (± SEM) normalized to control from n = 21 - 24 wells, N = 3. Effects ≤ 25% (2xSD of control; indicated by the grey area) are considered to be of limited toxicological relevance. Significant effects were determined by Welch's ANOVA and if exceeding 25% of control indicated by [a]=p < 0.05 for 0.5 h exposure compared to time-matched control, [b]=p < 0.05 for 24 h exposure compared to time-matched control, [c]=p < 0.05 for 48 h exposure compared to time-matched control, [d]=p < 0.05 for 120 h exposure compared to time-matched control.
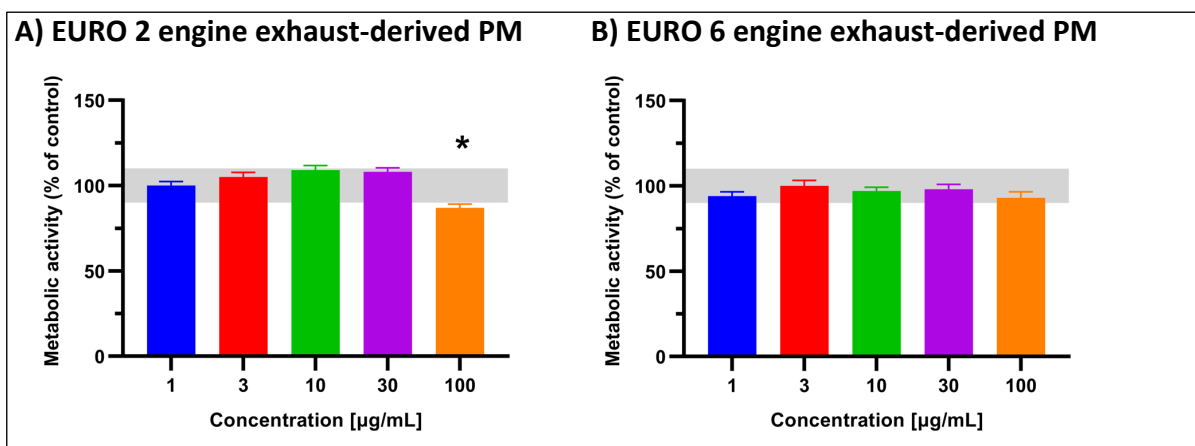
Figure 9: Effect of EURO 2 engine exhaust-derived PM (A) and EURO 6 engine exhaust-derived PM (B) on metabolic activity of rat primary cortical cultures after 120 h exposure. Cell viability data is presented as mean (± SD) normalized to control from n = 21 - 23 wells, N = 3. Effects ≤ 10% are of limited toxicological relevance and indicated by the grey area. Significant effects were determined by ordinary one-way ANOVA. *=$p < 0.05$ compared to control and exceeding 10%.

Non-volatile A0 and A20 show no consistent effect on neuronal (network) activity

Non-volatile UFP from A0-fuel reduced the MBR acute after 0.5 h and the MSR after 24 h and 48 h after exposure to 100 µg/mL, but no consistent effect is visible for the MNBR, or after 120 h of exposure (fig. 10A). As the effect on the MSR and MBR are not persistent, it is of limited toxicological relevance. Acute and prolonged exposure to 100 µg/mL Non-volatile UFP from A20-fuel resulted in a modest reduction of the MSR to 68.5% (p = <0.0001) and 58.7% (p = 0.0008) for 0.5 h and 120 h exposure, but no change in neuronal activity were detected for lower concentration or other parameters (fig. 10B). Subsequent Alamar Blue assay indicated that cell viability is not affected consistently by non-volatile A0 and non-volatile A20 (fig. 11).

Figure 10: Effect of non-volatile A0 (A) and non-volatile A20 (B) on neuronal (network) activity of rat primary cortical cultures. Effects on neuronal activity were assessed after 0.5 h, 24 h, 48 h and 120 h exposure. Mean Spike Rate (MSR), Mean Burst Rate (MBR), and Mean Network Burst Rate (MNBR) are presented as mean treatment ratio (± SEM) normalized to control from n = 20 - 24 wells, N = 3. Effects ≤ 25% (2xSD of control; indicated by the grey area) are considered to be of limited toxicological relevance. Significant effects were determined by Welch's ANOVA and if exceeding 25% of control indicated by [a]=p < 0.05 for 0.5 h exposure compared to time-matched control, [b]=p < 0.05 for 24 h exposure compared to time-matched control, [c]=p < 0.05 for 48 h exposure compared to time-matched control, [d]=p < 0.05 for 120 h exposure compared to time-matched control.

Figure 11: Effect of non-volatile A0 (A) and non-volatile A20 (B) on metabolic activity of rat primary cortical cultures after 120 h exposure. Cell viability data is presented as mean (± SD) normalized to control from n = 21 - 24 wells, N = 3. Effects ≤ 10% are of limited toxicological relevance and indicated by the grey area. Significant effects were determined by ordinary one-way ANOVA. *=p < 0.05 compared to control and exceeding 10%.

SVOC A0 and SVOC A20 decrease neuronal activity and cell viability

The SVOC A0 and A20 fractions are the UFP fractions of the A0- and A20-fuel exhaust in which the semivotalic organic compounds, which are in between the particle and the gaseous phase, are collected. Therefore, this group does not consist of the particles that we see in other sample groups. MSR and MBR were dose-dependently reduced following acute exposure (0.5 h) to 10 L/mL or 4 L/mL SVOC A0 to 63.3% (p = <0.0001) and 69.5% (p = 0.0002), respectively (fig. 12A). While the reduction remained for 20 L/mL, cells exposed to a concentration below 20 L/mL exhibits unaffected MSR and MBR for 24 h – 120 h exposure indicating recovery of the neuronal activity (fig. 12B). An acute reduction of the MSR and MBR was also observed for cells exposed to 10 L/mL SVOC A20 (71.7%, p = 0.0324 and 35.1%), but in contrast to the SVOC A0 exposed cells, neuronal activity parameters remained significantly decreased. After prolonged exposure, MBR was also reduced by lower doses of SVOC A20 (2 and 4 L/mL). However, data on metabolic activity suggest that SVOC A0 and SVOC A20 induced cell death with SVOC A20 being more potent. Cell viability was reduced to 75.0% and 50.0% for 10 and 20 L/mL SVOC A0 resp. (p = <0.0001 for both) and to 34.0% and 3.0% for 10 and 20 L/mL SVOC A20 resp. (p = <0.0001 for both) (fig. 13).
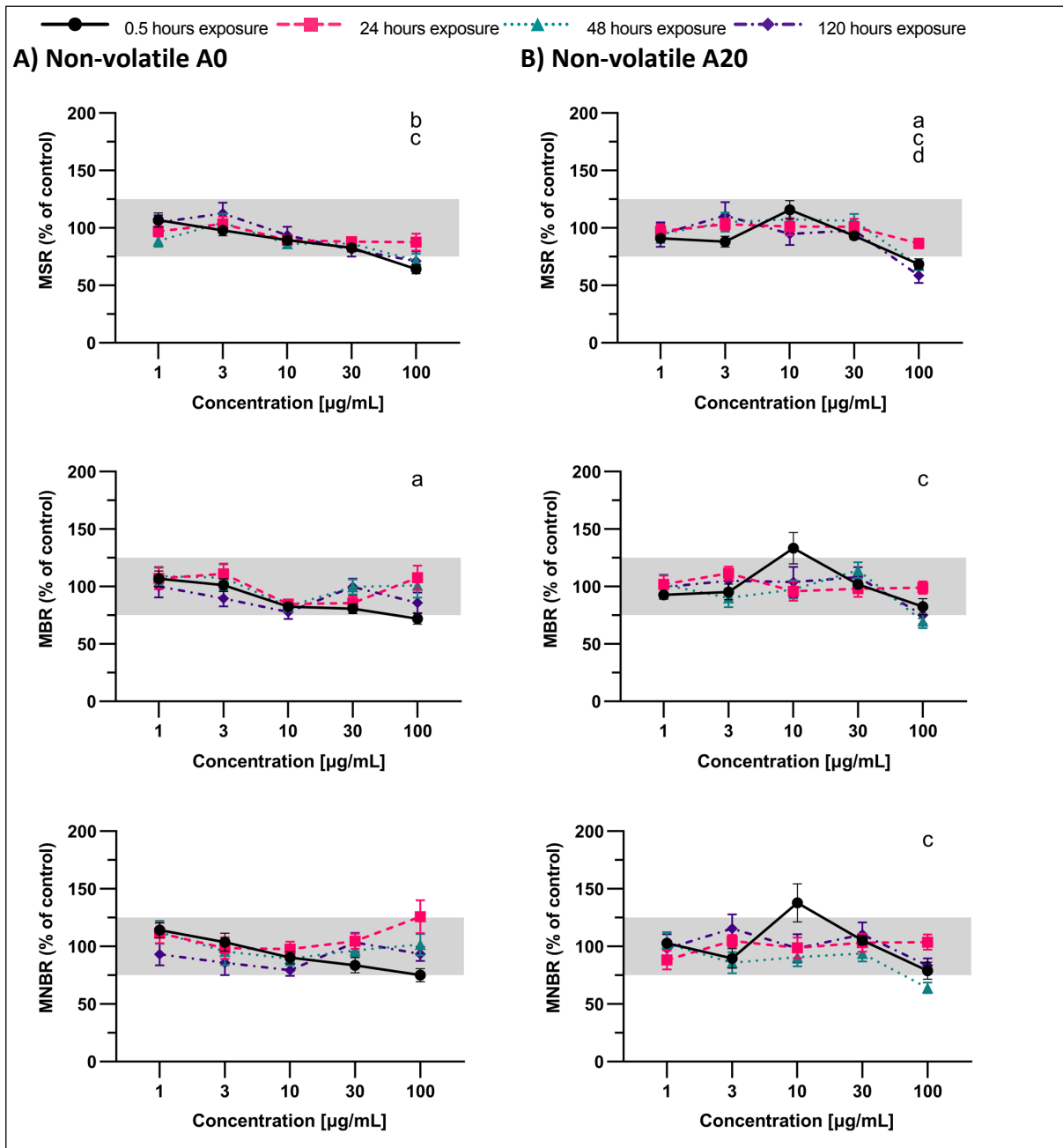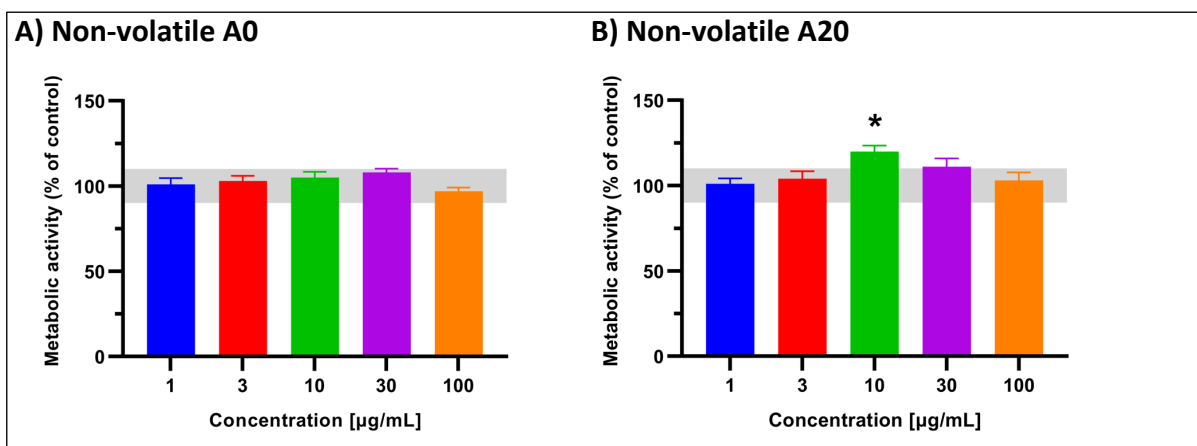
Figure 12: Effect of SVOC A0 (A) and SVOC A20 (B) on neuronal (network) activity of rat primary cortical cultures. Effects on neuronal activity were assessed after 0.5 h, 24 h, 48 h and 120 h exposure. Mean Spike Rate (MSR), Mean Burst Rate (MBR), and Mean Network Burst Rate (MNBR) are presented as mean treatment ratio (± SEM) normalized to control from n = 19 - 24 wells, N = 3. Effects ≤ 25% (2xSD of control; indicated by the grey area) are considered to be of limited toxicological relevance. Significant effects were determined by Welch's ANOVA and if exceeding 25% of control indicated by [a]=$p < 0.05$ for 0.5 h exposure compared to time-matched control, [b]=$p < 0.05$ for 24 h exposure compared to time-matched control, [c]=$p < 0.05$ for 48 h exposure compared to time-matched control, [d]=$p < 0.05$ for 120 h exposure compared to time-matched control.
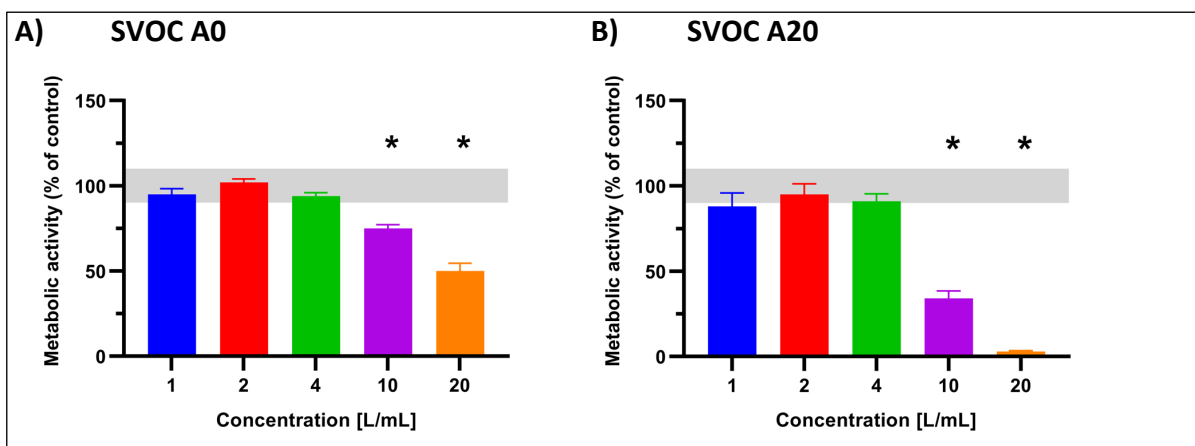
Figure 13: Effect of SVOC A0 (A) and SVOC A20 (B) on metabolic activity of rat primary cortical cultures after 120 h exposure. Cell viability data is presented as mean (± SD) normalized to control from n = 21 - 24 wells, N = 3. Effects ≤ 10% are of limited toxicological relevance and indicated by the grey area. Significant effects were determined by ordinary one-way ANOVA. *=p < 0.05 compared to control and exceeding 10%.

Size distribution

The size distribution was expressed as the D50 value, which displayed the median of hydrodynamic diameter of the samples (Table 3). Next to the samples, the D50 value of glutamate-free culture medium and diesel in H_2O were analysed. The glutmate-free medium was indicative for the background of the medium. Comparing the D50 of the Diesel measurements perfomed in H_2O and glutamate-free culture medium shows the impact of the culture medium on the hydrodynamic diameter measurement of the UFP. The difference of diesel in H_2O and diesel in glutamate-free culture medium indicate that the medium increases the hydrodynamic diameter. As expected, blank extract, SVOC A0 and SVOC A20 showed no apparent difference from the glutamate-free culture medium, thus indication that no solid particles were detected by the DLS. Also for EURO 6-compliant engine exhaust-derived PM, the DLS measurement did not detect particles. Diesel and biodiesel exhaust-derived PM, EURO 2-compliant engine exhaust-derived PM, and non-volatile A20 showed an D50 value falling in the PM2.5 size range, and the D50 value of non-volatile A0 falls into the UFP size range.

Table 3: Hydrodynamic diameter of the samples. Data is presented as D50 value (±SD)

Sample ID	D50 value (nm)	Sample concentration
Glutamate-free culture medium (equivalent to the background)	7.4 ± 0.3	-
Diesel in H_2O	167.8 ± 94.6	100 µg/mL
Blank extract	8.3 ± 0.6	100 µg/mL
Copper oxide particles	362.4 ± 25.4	100 µg/mL
Diesel	270.2 ± 15.1	100 µg/mL
Biodiesel	245.7 ± 139.5	100 µg/mL
EURO 2 diesel	532.5 ± 168.3	100 µg/mL
EURO 6 diesel	7.6 ± 0.3	100 µg/mL
PM A0	97.1 ± 152.9	10 L/mL
PM A20	405.9 ±15.6	10 L/mL
SVOC A0	7.6 ± 0.3	10 L/mL
SVOC A20	7.1 ± 1.1	10 L/mL

Discussion

In this study, various fractions (non-volatile and semi-volatile organic compounds) of traffic-derived PM, as well as reference materials, were screened for their effects on neuronal (network) function in rat primary cortical cultures using MEA recordings aiming to compare the potential neurotoxic hazard of these PMs. One of the main obeservations was that common rail engine diesel generator diesel exhaust-derived PM reduces neuronal activity more, both time- and dose-dependent, than biodiesel exhaust-derived PM suggesting the PM originating from diesel exhaust is more neurotoxic. For heavy-duty engines, SVOC generated using high-aromatic (A20) diesel exhibited more neurotoxic potential than SVOC collected from the same engine when fueled with low-aromatic (A0). However, high dose exposure to SVOC was associated with cytotoxicicity and therefore at high dose no specific neurotoxicity occured. Further, the non-cytotoxic SVOC PM fraction originating from A20 and A0 diesel reduced neuronal activity to a greater extent than their corresponding non-volatile PM fraction. Finally, carbon particles, blank extract, EURO 2 and EURO 6 engine exhaust-derived PM showed no consistent (time- and dose-dependent) decrease in neuronal activity and cytotoxicity, while the copper oxide particles showed significant cytotoxic potential resulting in decreased neuronal activty.

The particle size of the samples is measured with the DLS and expressed in the D50 value for the median of the hydrodynamic diameter. For the Blank extract, SVOC A0, SVOC A20 and the EURO 6 compliant engine exhaust-derived PM, no particles were detected that deviated from the D50 value of the glutamate-free culture medium. These samples indeed did not generate mass as with the other samples and were expressed in exhaust volume or the corresponding mass relative to the other samples. Diesel and biodiesel exhaust-derived PM, EURO 2 compliant engine exhaust-derived PM, PM A0, PM A20 and copper oxide particles did show a D50 value differing from the glutamate-free culture medium, ranging from 97 to 532 nm. The D50 values of diesel in medium was far greater than diesel in H_2O, indicating that the medium increases the hydrodynamic diameter. Nanoparticles in a biological environment form a corona that could be measured as part of the hydrodynamic diameter in the DLS (Li & Lee, 2020). Furthermore, the chemicals that are attached on the surface of the particles could interact with the medium, further increasing the measured hydrodynamic diameter. Therefore it is possible that the medium causes the hydrodynamic diameter to be measured greater than the actual particle diameter and that these particles fall within the UFP size range. Furthermore, the EURO 2 compliant engine exhaust-derived PM showed the greatest hydrodynamic diameter of 532 ± 168 nm. This sample appeared to strongly and inconsistenly clump together, possibly leading to irregular particles and high standard deviation.

Diesel and biodiesel exhaust-derived PM

By exposing rat cortical cultures on the MEA acutely and subchronically, the difference in neuronal activity of diesel- and biodiesel-derived PM was analyzed. These results showed that biodiesel exhaust-derived PM, which was the result of the combustion of diesel supplemented with 20% biodiesel, had a less detrimental effect on neuronal activity than its diesel-only counterpart.

Previous research showed contradicting results on the decrease of known toxic components in biodiesel exhaust compared to PM derived from regular diesel. In several studies

on the chemical composition of engine exhaust, exchanging diesel fuel to biodiesel reduced the concentration of known toxicants, such as PAH and metals, in engine exhaust-derived PM (Karavalakis et al., 2017; Tsai et al., 2011). Furthermore, Karavalakis et al. saw that the addition of biodiesel to diesel fuel decreased the oxidative capacity and cellular reactivity of the exhaust. Contrastingly, other studies showed that the biodiesel blends in various ratios, as opposed to diesel-only fuel, induced adverse effects in non-neuronal cell lines, including increased inflammatory response, oxidative activity, and cytotoxicity (Fukagawa et al., 2013; Gerlofs-Nijland et al., 2013; Grigoratos et al., 2014). A rat inhalation study by Valand et al. (2018) focused specifically on neuronal integrity between diesel and various biodiesel blend exposed animal after 7- and 28-day exposure. Only mild and no consistent alterations between different exposure groups were present for gene expression of genes that were related to redox responses (Cat, Gpx1, Gsr, Sod1, Sod2), genes associated with inflammation (Ccl3, Nfkb1, Il18) and histopathology of the frontal cortex and hippocampus. Further, no conclusive research has been done on the difference in the effect of diesel and biodiesel exhaust-derived PM on neurophysiology, neurotransmission, receptor activation etc. Hence, no consensus is reached on the difference between diesel and biodiesel engine exhaust in literature, more specifically on the fractions of PM. Nevertheless, our results support the hypothesis that biodiesel has less adverse health effects on the CNS.

Aromatic compounds in exhaust-derived PM

After combustion of the low aromatic A0 and the high aromatic A20 fuels, the exhaust was collected in fractions of non-volatile UFP and SVOC UFP per fuel. The non-volatile fractions of A0 and A20 induced no relevant changes in neuronal activity. For both SVOC UFP samples derived from A0 and A20 fuel, our data showed clear dose- and time-dependent reduction of neuronal activity. However, the effects seen for SVOC A20 were far greater than SVOC A0-induced changes indicating that the A20-derived samples exhibit higher neurotoxic potency. SVOC are a fraction of engine exhaust that fluctuates between the particle and gaseous phase and contain, amongst others, the known toxicant group of PAH. This can explain that SVOC, and especially A20, disrupt neuronal activity, because the concentration of potential toxic aromatic compounds is also expected to be far greater than for non-volatile UFP. However, it is still expected that a fraction of the SVOC would coat and be present in the non-volatile UFP, as they would retain in the particle state upon collection.

The SVOC UFP fractions did not contain equal amounts of mass as non-volatile UFP from the A0 and A20 fuels did because they are partly gaseous. Therefore, SVOC UFP fractions were not collected on filters, but on absorption tubes from which the weight of collected sample could not be determined. On the other hand, the volume of exhaust from which the SVOC UFP was collected was known. Therefore, the SVOC UFP were exposed in L/mL rather than mg/mL, with the highest dose of 20 L/mL instead of 100 mg/mL as for the non-volatile fractions. To correctly compare these fractions, the exposure doses of the non-volatile UFP were recalculated to equal units in L/mL. As the collected volume for 1 mg collected non-volatile UFP was 0.38 and 0.56 m^3/mg for the A0 and A20, respectively, the highest doses were equal to 37.7 and 55.8 L/mL. So compared to the SVOC UFP fraction, the exposed doses were ca two times higher than the dose for the SVOC, making the SVOC UFP fractions from A0 and A20 fuel even more potent relatively to the non-volatile UFP fractions.

Possible mechanism of toxicity from SVOC exposure

The cytotoxicity was measured to distinguish whether inhibition of neurological activity is due to specifc interaction with cellular processes important for neuronal signalling, or general cytotoxicity such as apoptosis or necrosis, which would also result in lower neuronal activity. Both SVOC UFP fractions of A0 and A20 showed cytotoxicity for the dose that lowered the neuronal activity. This indicates that the decrease in neuronal activity subchronically was more related to general cellular processes, rather than the effect on specific neurological processes. However, also acute inhibition of the activity was observed which is unlikely a result of cytotoxicity indicating that SVOC do exhibit specific neurotoxicity. It is suggested to ensure that the SVOC did not affect cell viability after acute exposure. Possible mechanisms that could acutely affect neurological function include changes in receptor activation and calcium concentrations in neuronal cells (Brinchmann et al., 2018; Mayati et al., 2012). The study by Mayati et al. showed an acute (20-25 min) increase of intracellular calcium concentration ($[Ca^{2+}]_i$) after exposure to PAH on human microvascular endothelial cells, independent of the aryl hydrocarbon receptor (AhR) pathway. Similar results are seen in the study of Brinchmann et al., which shows an acute (30 min) increase of $[Ca^{2+}]_i$ after exposure to the organic fractions of diesel engine particles on human microvascular endothelial cells. The effect of these fractions, which incorporate the SVOC, were hypothesized to be dependent on AhR signalling and the transient receptor potential channel (TRPC). Both AhR and TRPC are present in rat cortices and human cell lines, and function as ligand activated transcription factor for xenobiotics and voltage-independent cation channel respectively (Fowler et al., 2007; Jin et al., 2004; Roedding et al., 2009; Xu et al., 2016). These processes potentially affect receptor (in)activation and calcium homeostasis, processes which are essential for neuronal signaling (J. Huang et al., 2011; Juricek & Coumoul, 2018), but more specific investigations are necessary to reveal which compounds in the mix of SVOC are responsible for the acute neurotoxicity and which cellular mechanisms are disturbed.

Reference materials

The results of the generated UFP carbon and copper oxide analysis indicate that both samples did not induce specific neurotoxicity. The use of the MEA is previously shown to be successful for the assessment of the neurotoxic hazard of nanoparticles (Strickland et al., 2015, 2016). The carbon particles showed no decrease in neuronal activity. The results did show a decrease in cell viability, but this is most likely due to interference of the carbon particles at the photospectometer used for the Alamar Blue assay rather than cytotoxicity of the sample (Breznan et al., 2015). Furthermore, the copper oxide particles range did decrease neuronal activity at the highest dose of 1 μg/mL. However, this decrease correlates with the cell viability assay data indicating cytotoxicity which was even observed at a lower dose of 0.3 μg/mL. A study from Karlsson et al. (2008) on the effect of nanoparticles on human epithelial lung cells confirms our results. In this study, the copper oxide nanoparticles induced cytotoxicity at a concentration of 80 μg/mL after 18 h resulting from DNA damage and oxidative lesions, which were absent for carbon nanoparticles.

A rat study performed by Oberdörster et al. (2004) confirmed that carbon black UFP can translocate into the olfactory bulb and therefore the CNS, but the effect of these particles on the CNS remains unknown. Exposure to only carbon particles did not inhibit neuronal activity, which substantiates that solid carbon UFP in engine exhaust did not act as the toxic component itself.

Furthermore, the solid carbon UFP could still act as a carrier for other toxicants on its surface (Gerde et al., 2001).

In contrast, several studies on copper oxide UFP showed that it could affect cells in the CNS (Bulcke et al., 2013; Bulcke & Dringen, 2016; Fahmy et al., 2020; Zhang et al., 2012). These studies focus mostly on the induction of oxidative stress and decrease in cell viability, which underpins our results that the effect of copper oxide UFP is related to cytotoxicity. However, the study by Zhang et al. (2012) also found that the secretion of neurotransmitters changed in some brain regions, suggesting that copper UFP interferes in specific neurological processes. Furthermore, these copper nanoparticles are hypothesized by Zhang et al. (2012) to affect the dopaminergic pathways, which are absent in our rat primary cortex cultures and explains that this effects was not present for the results of this study (Hondebrink et al., 2016).

Future research

There is still a lack of knowledge on the composition of diesel exhaust in particular the related emitted PM. Although multiple studies researched the size distribution and chemical composition of diesel exhaust (Alam et al., 2016; Bünger et al., 2000; Popovicheva et al., 2015; Tsolakis, 2006), the variation in size distribution and especially chemical composition among studies is great because of several differences during sample generation, collection and extraction including fuel and engine types used, aftertreatment methods (e.g. diesel particle filter, diesel oxidation catalyst and selective catalytic reduction), engine load and temperatures during sample collection (Guan et al., 2015; Hays et al., 2017; Jiang et al., 2019; Martin et al., 2017; Zerboni et al., 2022). For instance, Zielinska et al. (2004) discovered that a lower temperature lead to an eight times increase of organic carbon in diesel exhaust emission. In our research, two different institutions, RIVM and UEF, with different circumstances and protocols provided the test samples. The diesel and biodiesel exhaust-derived PM data showed well-defined dose-effect curves that were not seen for the other non-volatile test samples collected on filters, which could be partly due to the different conditions and protocols used by RIVM as opposed to UEF. This variation will be even greater for comparisons between completely different studies. The use of standardized protocols for the combustion and collection of samples could be a way to tackle this variation. However, the options for fuel types, engine types etc. are endless and the same conditions are not always available worldwide.

Another point of interest when interpreting the results, is the unit in which the dose is expressed. The mass of collected PM per volume in the wells on the MEA was used to obtain exposure doses, as they were provided in vials with a known mass content. An advantage to this method is that the effect of a specific dose on neuronal activity would be clear, as this is the method that is generally applied with single chemicals. However, our samples are composed of complex mixtures collected from exhaustion from an engine. Therefore, relating our exposure doses to e.g. the elapsed time of sampling or the volume of fuel that was used to collect the samples could facilitate the comparison to a more realistic exposure. Additionally, the different diesel fuels or engines used in this study could lead to a higher or lower mass of PM, but as we expose per unit of mass, this consideration is not included in our experiments and may affect their outcome. In a study by Tsai et al. (2011), a 20% biodiesel blend lowered the mass of PM by 30% as opposed to diesel. If this reduction is present in our study, it could lead to a longer runtime of the engine to obtain the same dose in mass per volume. This would lead to a lower exposure per

volume of fuel or driven distance, suggesting that biodiesel exhaust-derived PM is even less toxic than our results indicate. An experiment including the measurement of the mass of collected PM per volume of exhaust or fuel should define if a reduction of PM is present and would provide results that are easier extrapolated to human exposures. To better directly compare the toxicity of fuel exhaust to realistic human exposure, expressing concentrations in driven distance for the amount of PM that is collected would be suitable. This way, the efficiency of the engine and fuel source are also taking into account, keeping in mind that different fuels and engines also provide different levels of energy conversion.

Working with doses that are representative for realistic exposure conditions to PM in urban areas is critical for risk assessment. In the present study, doses ranging from 1-100 µg/mL and 1-20 L/mL were selected for *in vitro* investigations to compare the various samples for neuronal (network) activity and cytotoxicity after exposure. The amount of PM that reaches the brain remains to be determined, but a study discovered that an estimate of 0.01-0.001% of inhaled iridium and carbon nanoparticles were found in the brain after 24 h exposure (Kreyling et al., 2009). Furthermore, a study on the *in vitro* and *in vivo* effect of diesel exhaust UFP derived that, based on the estimation of Kreyling et al. (2009) and their *in vivo* model using 0.5 and 2 mg/m^3 inhalation exposure of diesel exhaust UFP to rats, an *in vitro* exposure doses range of 5-50 µg/mL falls within the current estimates of what may reach the brain. Various studies use comparable doses for *in vitro* exposure to neuronal cell lines, ranging from 1-50 µg/mL (Campbell et al., 2014; Gillespie et al., 2013; Morgan et al., 2011). Comparing these doses to realistic exposures remains complicated as UFP levels are not commonly measured. As mentioned before, UFP are not monitored by the EU and limit values are missing (European Parliament et al., 2021). Furthermore, spatial variations between UFP are weakly represented by PM2.5 measurements (Weichenthal et al., 2020) and UFP is better expressed in particle number concentration than PM mass used for PM2.5 and PM10 (de Jesus et al., 2019). Therefore, the measurements and limits for PM2.5 and PM10 in ambient air deriving from diesel engine exhaust do not correctly translate to the exposure to UFP and the associated health risk.

Conclusion

The current research was done to determine whether diesel engine-derived exhaust PM affect neuronal (network) activity and give insight into which fractions could pose the most harm. To conclude, the current study shows a time- and dose-dependent decrease of neuronal activity after exposure to diesel and biodiesel exhaust-derived PM, with diesel exhaust-derived PM showing a higher potency to exert harm. Also, the SVOC fraction seems to be more detrimental than the non-volatile PM fraction, albeit the observed subchronic effects are partly due to general cytotoxic than specifically neurotoxic. Furthermore, the results show that UFP exhibit neurotoxic potential that possibly harm neuronal function. Therefore, more attention for the impact of exposure to UFP, and specifically the SVOC fraction, is necessary. This novel knowledge on the neurotoxic hazard of different fractions within exhaust-derived PM opens the floor for more targeted research on the mechanisms that affect the neurotoxicity of UFP.

References

Alam, M. S., Zeraati-Rezaei, S., Stark, C. P., Liang, Z., Xu, H., & Harrison, R. M. (2016). The characterisation of diesel exhaust particles-composition, size distribution and partitioning. *Faraday Discussions*, *189*, 69–84. https://doi.org/10.1039/c5fd00185d

Alemany, S., Crous-Bou, M., Vilor-Tejedor, N., Milà-Alomà, M., Suárez-Calvet, M., Salvadó, G., Cirach, M., Arenaza-Urquijo, E. M., Sanchez-Benavides, G., Grau-Rivera, O., Minguillon, C., Fauria, K., Kollmorgen, G., Domingo Gispert, J., Gascón, M., Nieuwenhuijsen, M., Zetterberg, H., Blennow, K., Sunyer, J., & Luis Molinuevo, J. (2021). Associations between air pollution and biomarkers of Alzheimer's disease in cognitively unimpaired individuals. *Environment International*, *157*. https://doi.org/10.1016/J.ENVINT.2021.106864

Block, M. L., & Calderón-Garcidueñas, L. (2009). Air pollution: mechanisms of neuroinflammation and CNS disease. *Trends in Neurosciences*, *32*(9), 506–516. https://doi.org/10.1016/j.tins.2009.05.009

Bräuner, E. V., Forchhammer, L., Möller, P., Simonsen, J., Glasius, M., Wåhlin, P., Raaschou-Nielsen, O., & Loft, S. (2007). Exposure to ultrafine particles from ambient air and oxidative stress-induced DNA damage. *Environmental Health Perspectives*, *115*(8), 1177–1182. https://doi.org/10.1289/EHP.9984

Breznan, D., Das, D., MacKinnon-Roy, C., Simard, B., Kumarathasan, P., & Vincent, R. (2015). Non-specific interaction of carbon nanotubes with the resazurin assay reagent: Impact on in vitro assessment of nanoparticle cytotoxicity. *Toxicology in Vitro*, *29*(1), 142–147. https://doi.org/10.1016/J.TIV.2014.09.009

Brinchmann, B., Le Ferrec, E., Podechard, N., Lagadic-Gossmann, D., Shoji, K., Penna, A., Kukowski, K., Kubátová, A., Holme, J., & Øvrevik, J. (2018). Lipophilic Chemicals from Diesel Exhaust Particles Trigger Calcium Response in Human Endothelial Cells via Aryl Hydrocarbon Receptor Non-Genomic Signalling. *International Journal of Molecular Sciences*, *19*(5), 1429. https://doi.org/10.3390/ijms19051429

Bulcke, F., & Dringen, R. (2016). Handling of Copper and Copper Oxide Nanoparticles by Astrocytes. *Neurochemical Research*, *41*(1–2), 33–43. https://doi.org/10.1007/s11064-015-1688-9

Bulcke, F., Thiel, K., & Dringen, R. (2013). Uptake and toxicity of copper oxide nanoparticles in cultured primary brain astrocytes. *Nanotoxicology*, *8*(7), 1–11. https://doi.org/10.3109/17435390.2013.829591

Bünger, J., Krahl, J., Baum, K., Schröder, O., Müller, M., Westphal, G., Ruhnau, P., Schulz, T. G., & Hallier, E. (2000). Cytotoxic and mutagenic effects, particle size and concentration analysis of diesel engine emissions using biodiesel and petrol diesel as fuel. *Archives of Toxicology*, *74*(8), 490–498. https://doi.org/10.1007/S002040000155

Calderón-Garcidueñas, L., Stommel, E. W., Rajkumar, R. P., Mukherjee, P. S., & Ayala, A. (2021). Particulate Air Pollution and Risk of Neuropsychiatric Outcomes. What We Breathe, Swallow, and Put on Our Skin Matters. *International Journal of Environmental Research and*

Public Health, *18*(21), 11568. https://doi.org/10.3390/ijerph182111568

Campbell, A., Daher, N., Solaimani, P., Mendoza, K., & Sioutas, C. (2014). Human brain derived cells respond in a type-specific manner after exposure to urban particulate matter (PM). *Toxicology in Vitro*, *28*(7), 1290–1295. https://doi.org/10.1016/j.tiv.2014.06.015

Campbell, A., Oldham, M., Becaria, A., Bondy, S. C., Meacher, D., Sioutas, C., Misra, C., Mendez, L. B., & Kleinman, M. (2005). Particulate Matter in Polluted Air May Increase Biomarkers of Inflammation in Mouse Brain. *NeuroToxicology*, *26*(1), 133–140. https://doi.org/10.1016/j.neuro.2004.08.003

Charlesworth, P., Cotterill, E., Morton, A., Grant, S. G. N., & Eglen, S. J. (2015). Quantitative differences in developmental profiles of spontaneous activity in cortical and hippocampal cultures. *Neural Development*, *10*(1), 1. https://doi.org/10.1186/S13064-014-0028-0

Chen, H., Kwong, J. C., Copes, R., Hystad, P., van Donkelaar, A., Tu, K., Brook, J. R., Goldberg, M. S., Martin, R. V., Murray, B. J., Wilton, A. S., Kopp, A., & Burnett, R. T. (2017). Exposure to ambient air pollution and the incidence of dementia: A population-based cohort study. *Environment International*, *108*, 271–277. https://doi.org/10.1016/J.ENVINT.2017.08.020

Chen, J., & Hoek, G. (2020). Long-term exposure to PM and all-cause and cause-specific mortality: A systematic review and meta-analysis. *Environment International*, *143*, 105974. https://doi.org/10.1016/j.envint.2020.105974

Chiappalone, M., Vato, A., Berdondini, L., Koudelka-Hep, M., & Martinoia, S. (2007). Network dynamics and synchronous activity in cultured cortical neurons. *International Journal of Neural Systems*, *17*(2), 87–103. https://doi.org/10.1142/S0129065707000968

Cohen, A. J., Brauer, M., Burnett, R., Anderson, H. R., Frostad, J., Estep, K., Balakrishnan, K., Brunekreef, B., Dandona, L., Dandona, R., Feigin, V., Freedman, G., Hubbell, B., Jobling, A., Kan, H., Knibbs, L., Liu, Y., Martin, R., Morawska, L., … Forouzanfar, M. H. (2017). Estimates and 25-year trends of the global burden of disease attributable to ambient air pollution: an analysis of data from the Global Burden of Diseases Study 2015. *The Lancet*, *389*(10082), 1907–1918. https://doi.org/10.1016/S0140-6736(17)30505-6

Costa, L. G., Cole, T. B., Coburn, J., Chang, Y.-C., Dao, K., & Roqué, P. J. (2017). Neurotoxicity of traffic-related air pollution. *NeuroToxicology*, *59*(3), 133–139. https://doi.org/10.1016/j.neuro.2015.11.008

de Jesus, A. L., Rahman, M. M., Mazaheri, M., Thompson, H., Knibbs, L. D., Jeong, C., Evans, G., Nei, W., Ding, A., Qiao, L., Li, L., Portin, H., Niemi, J. V., Timonen, H., Luoma, K., Petäjä, T., Kulmala, M., Kowalski, M., Peters, A., … Morawska, L. (2019). Ultrafine particles and PM2.5 in the air of cities around the world: Are they representative of each other? *Environment International*, *129*, 118–135. https://doi.org/10.1016/j.envint.2019.05.021

de Kok, T. M. C. M., Driece, H. A. L., Hogervorst, J. G. F., & Briedé, J. J. (2006). Toxicological assessment of ambient and traffic-related particulate matter: A review of recent studies. *Mutation Research/Reviews in Mutation Research*, *613*(2–3), 103–122. https://doi.org/10.1016/j.mrrev.2006.07.001

Dingemans, M. M. L., Schütte, M. G., Wiersma, D. M. M., de Groot, A., van Kleef, R. G. D. M., Wijnolts, F. M. J., & Westerink, R. H. S. (2016). Chronic 14-day exposure to insecticides or methylmercury modulates neuronal activity in primary rat cortical cultures. *NeuroToxicology*, *57*, 194–202. https://doi.org/10.1016/j.neuro.2016.10.002

Elder, A., Gelein, R., Silva, V., Feikert, T., Opanashuk, L., Carter, J., Potter, R., Maynard, A., Ito, Y., Finkelstein, J., & Oberdörster, G. (2006). Translocation of inhaled ultrafine manganese oxide particles to the central nervous system. *Environmental Health Perspectives*, *114*(8), 1172–1178. https://doi.org/10.1289/EHP.9030

European Parliament. (2008). Directive 2008/50/EC of the European Parliament and of the Council of 21 May 2008 on ambient air quality and cleaner air for Europe. In *Official Journal of the European Union* (Vol. 152). Official Journal of the European Union.

European Parliament, Directorate-General for Parliamentary Research Services, Karamfilova, E., & De La Trinidad Salvador Sanz, L. (2021). *EU policy on air quality: Implementation of selected EU legislation* (Issue January). European Parliament. https://doi.org/10.2861/808342

Fagundes, L. S., Fleck, A. D. S., Zanchi, A. C., Saldiva, P. H. N., & Rhoden, C. R. (2015). Direct contact with particulate matter increases oxidative stress in different brain structures. *Inhalation Toxicology*, *27*(10), 462–467. https://doi.org/10.3109/08958378.2015.1060278

Fahmy, H. M., Ali, O. A., Hassan, A. A., & Mohamed, M. A. (2020). *Biodistribution and toxicity assessment of copper nanoparticles in the rat brain*. https://doi.org/10.1016/j.jtemb.2020.126505

Fowler, M. A., Sidiropoulou, K., Ozkan, E. D., Phillips, C. W., & Cooper, D. C. (2007). Corticolimbic expression of TRPC4 and TRPC5 channels in the rodent brain. *PloS One*, *2*(6). https://doi.org/10.1371/JOURNAL.PONE.0000573

Fukagawa, N. K., Li, M., Poynter, M. E., Palmer, B. C., Parker, E., Kasumba, J., & Holmén, B. A. (2013). Soy biodiesel and petrodiesel emissions differ in size, chemical composition and stimulation of inflammatory responses in cells and animals. *Environmental Science and Technology*, *47*(21), 12496–12504. https://doi.org/10.1021/ES403146C/SUPPL_FILE/ES403146C_SI_001.PDF

Genc, S., Zadeoglulari, Z., Fuss, S. H., & Genc, K. (2012). The Adverse Effects of Air Pollution on the Nervous System. *Journal of Toxicology*, *2012*, 1–23. https://doi.org/10.1155/2012/782462

Gerber, L. S., van Melis, L. V. J., van Kleef, R. G. D. M., de Groot, A., & Westerink, R. H. S. (2021). Culture of Rat Primary Cortical Cells for Microelectrode Array (MEA) Recordings to Screen for Acute and Developmental Neurotoxicity. *Current Protocols*, *1*(6), 1–35. https://doi.org/10.1002/cpz1.158

Gerde, P., Muggenburg, B. A., Lundborg, M., & Dahl, A. R. (2001). The rapid alveolar absorption of diesel soot-adsorbed benzo[a]pyrene: bioavailability, metabolism and dosimetry of an inhaled particle-borne carcinogen. *Carcinogenesis*, *22*(5), 741–749. https://doi.org/10.1093/CARCIN/22.5.741

Gerlofs-Nijland, M. E., Totlandsdal, A. I., Tzamkiozis, T., Leseman, D. L. A. C., Samaras, Z., Låg, M., Schwarze, P., Ntziachristos, L., & Cassee, F. R. (2013). Cell toxicity and oxidative potential of engine exhaust particles: Impact of using particulate filter or biodiesel fuel blend. *Environmental Science and Technology*, *47*(11), 5931–5938. https://doi.org/10.1021/ES305330Y/SUPPL_FILE/ES305330Y_SI_002.PDF

Gerlofs-Nijland, M. E., van Berlo, D., Cassee, F. R., Schins, R. P. F. F., Wang, K., & Campbell, A. (2010). Effect of prolonged exposure to diesel engine exhaust on proinflammatory markers in different regions of the rat brain. *Particle and Fibre Toxicology*, *7*, 1–10. https://doi.org/10.1186/1743-8977-7-12

Ghio, A. J., Smith, C. B., & Madden, M. C. (2012). Diesel exhaust particles and airway inflammation. *Current Opinion in Pulmonary Medicine*, *18*(2), 144–150. https://doi.org/10.1097/MCP.0b013e32834f0e2a

Gillespie, P., Tajuba, J., Lippmann, M., Chen, L.-C., & Veronesi, B. (2013). Particulate matter neurotoxicity in culture is size-dependent. *NeuroToxicology*, *36*, 112–117. https://doi.org/10.1016/j.neuro.2011.10.006

Grigoratos, T., Fontaras, G., Kalogirou, M., Samara, C., Samaras, Z., & Rose, K. (2014). Effect of rapeseed methylester blending on diesel passenger car emissions – Part 2: Unregulated emissions and oxidation activity. *Fuel*, *128*, 260–267. https://doi.org/10.1016/j.fuel.2014.03.018

Guan, B., Zhan, R., Lin, H., & Huang, Z. (2015). *Review of the state-of-the-art of exhaust particulate filter technology in internal combustion engines*. https://doi.org/10.1016/j.jenvman.2015.02.027

Hamra, G. B., Guha, N., Cohen, A., Laden, F., Raaschou-Nielsen, O., Samet, J. M., Vineis, P., Forastiere, F., Saldiva, P., Yorifuji, T., & Loomis, D. (2014). Outdoor particulate matter exposure and lung cancer: A systematic review and meta-analysis. *Environmental Health Perspectives*, *122*(9), 906–911. https://doi.org/10.1289/EHP.1408092

Hays, M. D., Preston, W., George, B. J., George, I. J., Snow, R., Faircloth, J., Long, T., Baldauf, R. W., & McDonald, J. (2017). Temperature and Driving Cycle Significantly Affect Carbonaceous Gasand Particle Matter Emissions from Diesel Trucks. *Energy & Fuels : An American Chemical Society Journal*, *31*(10), 11034–11042. https://doi.org/10.1021/ACS.ENERGYFUELS.7B01446

Hesterberg, T. W., Long, C. M., Sax, S. N., Lapin, C. A., McClellan, R. O., Bunn, W. B., & Valberg, P. A. (2011). Particulate Matter in New Technology Diesel Exhaust (NTDE) is Quantitatively and Qualitatively Very Different from that Found in Traditional Diesel Exhaust (TDE). *Journal of the Air & Waste Management Association*, *61*(9), 894–913. https://doi.org/10.1080/10473289.2011.599277

Hoek, G., Krishnan, R. M., Beelen, R., Peters, A., Ostro, B., Brunekreef, B., & Kaufman, J. D. (2013). Long-term air pollution exposure and cardio-respiratory mortality: A review. *Environmental Health: A Global Access Science Source*, *12*(1), 43. https://doi.org/10.1186/1476-069X-12-

Hondebrink, L., Verboven, A. H. A., Drega, W. S., Schmeink, S., de Groot, M. W. G. D. M., van Kleef, R. G. D. M., Wijnolts, F. M. J., de Groot, A., Meulenbelt, J., & Westerink, R. H. S. (2016). Neurotoxicity screening of (illicit) drugs using novel methods for analysis of microelectrode array (MEA) recordings. *NeuroToxicology*, *55*, 1–9. https://doi.org/10.1016/j.neuro.2016.04.020

Huang, J., Du, W., Yao, H., & Wang, Y. (2011). TRPC Channels in Neuronal Survival. *TRP Channels*. https://www.ncbi.nlm.nih.gov/books/NBK92826/

Huang, L., Bohac, S. V., Chernyak, S. M., & Batterman, S. A. (2013). Composition and Integrity of PAHs, Nitro-PAHs, Hopanes and Steranes In Diesel Exhaust Particulate Matter. *Water, Air, and Soil Pollution*, *224*(8). https://doi.org/10.1007/S11270-013-1630-1

Jiang, H., Wu, G., Li, T., He, P., & Chen, R. (2019). *Characteristics of Particulate Matter Emissions from a Low-Speed Marine Diesel Engine at Various Loads*. https://doi.org/10.1021/acs.est.9b02341

Jin, D.-Q., Jung, J. W., Lee, Y. S., & Kim, J.-A. (2004). 2,3,7,8-Tetrachlorodibenzo-p-dioxin inhibits cell proliferation through arylhydrocarbon receptor-mediated G1 arrest in SK-N-SH human neuronal cells. *Neuroscience Letters*, *363*(1), 69–72. https://doi.org/10.1016/j.neulet.2004.03.047

Juricek, L., & Coumoul, X. (2018). The Aryl Hydrocarbon Receptor and the Nervous System. *International Journal of Molecular Sciences*, *19*(9). https://doi.org/10.3390/IJMS19092504

Kanayama, Y., Enomoto, S., Irie, T., & Amano, R. (2005). Axonal transport of rubidium and thallium in the olfactory nerve of mice. *Nuclear Medicine and Biology*, *32*(5), 505–512. https://doi.org/10.1016/j.nucmedbio.2005.03.009

Karavalakis, G., Gysel, N., Schmitz, D. A., Cho, A. K., Sioutas, C., Schauer, J. J., Cocker, D. R., & Durbin, T. D. (2017). Impact of biodiesel on regulated and unregulated emissions, and redox and proinflammatory properties of PM emitted from heavy-duty vehicles. *Science of The Total Environment*, *584–585*, 1230–1238. https://doi.org/10.1016/j.scitotenv.2017.01.187

Karlsson, H. L., Cronholm, P., Gustafsson, J., & Möller, L. (2008). Copper oxide nanoparticles are highly toxic: A comparison between metal oxide nanoparticles and carbon nanotubes. *Chemical Research in Toxicology*, *21*(9), 1726–1732. https://doi.org/10.1021/TX800064J/ASSET/IMAGES/TX800064J.SOCIAL.JPEG_V03

Khreis, H., Ramani, T., de Hoogh, K., Mueller, N., Rojas-Rueda, D., Zietsman, J., & Nieuwenhuijsen, M. J. (2019). Traffic-related air pollution and the local burden of childhood asthma in Bradford, UK. *International Journal of Transportation Science and Technology*, *8*(2), 116–128. https://doi.org/10.1016/j.ijtst.2018.07.003

Kim, D., Chen, Z., Zhou, L.-F., & Huang, S.-X. (2018). Air pollutants and early origins of respiratory diseases. *Chronic Diseases and Translational Medicine*, *4*(2), 75–94. https://doi.org/10.1016/j.cdtm.2018.03.003

Kreyling, W. G., Semmler-Behnke, M., Seitz, J., Scymczak, W., Wenk, A., Mayer, P., Takenaka, S., & Oberdrster, G. (2009). Size dependence of the translocation of inhaled iridium and carbon nanoparticle aggregates from the lung of rats to the blood and secondary target organs. *Https://Doi-Org.Proxy.Library.Uu.Nl/10.1080/08958370902942517*, *21*(SUPPL. 1), 55–60. https://doi.org/10.1080/08958370902942517

Kwon, H.-S. S., Ryu, M. H., & Carlsten, C. (2020). Ultrafine particles: unique physicochemical properties relevant to health and disease. *Experimental & Molecular Medicine*, *52*(3), 318–328. https://doi.org/10.1038/s12276-020-0405-1

Legendy, C. R., & Salcman, M. (1985). Bursts and recurrences of bursts in the spike trains of spontaneously active striate cortex neurons. *Journal of Neurophysiology*, *53*(4), 926–939. https://doi.org/10.1152/jn.1985.53.4.926

Lelieveld, J., Klingmüller, K., Pozzer, A., Pöschl, U., Fnais, M., Daiber, A., & Münzel, T. (2019). Cardiovascular disease burden from ambient air pollution in Europe reassessed using novel hazard ratio functions. *European Heart Journal*, *40*(20), 1590–1596. https://doi.org/10.1093/eurheartj/ehz135

Levesque, S., Surace, M. J., McDonald, J., & Block, M. L. (2011). Air pollution & the brain: Subchronic diesel exhaust exposure causes neuroinflammation and elevates early markers of neurodegenerative disease. *Journal of Neuroinflammation*, *8*(1), 105. https://doi.org/10.1186/1742-2094-8-105

Li, Y., & Lee, J. S. (2020). Insights into Characterization Methods and Biomedical Applications of Nanoparticle–Protein Corona. *Materials 2020, Vol. 13, Page 3093*, *13*(14), 3093. https://doi.org/10.3390/MA13143093

Manigrasso, M., Costabile, F., Liberto, L. Di, Gobbi, G. P., Gualtieri, M., Zanini, G., & Avino, P. (2020). Size resolved aerosol respiratory doses in a Mediterranean urban area: From PM10 to ultrafine particles. *Environment International*, *141*, 105714. https://doi.org/10.1016/j.envint.2020.105714

Mannucci, P. M., Harari, S., & Franchini, M. (2019). Novel evidence for a greater burden of ambient air pollution on cardiovascular disease. *Haematologica*, *104*(12), 2349–2357. https://doi.org/10.3324/haematol.2019.225086

Martin, N., Lombard, M., Jensen, K. R., Kelley, P., Pratt, T., & Traviss, N. (2017). Effect of biodiesel fuel on "real-world", nonroad heavy duty diesel engine particulate matter emissions, composition and cytotoxicity. *Science of The Total Environment*, *586*(3), 409–418. https://doi.org/10.1016/j.scitotenv.2016.12.041

Mayati, A., Le Ferrec, E., Lagadic-Gossmann, D., & Fardel, O. (2012). Aryl hydrocarbon receptor-independent up-regulation of intracellular calcium concentration by environmental polycyclic aromatic hydrocarbons in human endothelial HMEC-1 cells. *Environmental Toxicology*, *27*(9), 556–562. https://doi.org/10.1002/TOX.20675

McCormick, R. L., Williams, A., Ireland, J., & Hayes, R. R. (2006). *Effects of Biodiesel Blends on Vehicle Emissions: Fiscal Year 2006 Annual Operating Plan Milestone 10.4.*

https://doi.org/10.2172/894987

Morgan, T. E., Davis, D. A., Iwata, N., Tanner, J. A., Snyder, D., Ning, Z., Kam, W., Hsu, Y. T., Winkler, J. W., Chen, J. C., Petasis, N. A., Baudry, M., Sioutas, C., & Finch, C. E. (2011). Glutamatergic Neurons in Rodent Models Respond to Nanoscale Particulate Urban Air Pollutants in Vivo and in Vitro. *Environmental Health Perspectives*, *119*(7), 1003. https://doi.org/10.1289/EHP.1002973

Oberdörster, G., Oberdörster, E., & Oberdörster, J. (2005). Nanotoxicology: An Emerging Discipline Evolving from Studies of Ultrafine Particles. *Environmental Health Perspectives*, *113*(7), 823–839. https://doi.org/10.1289/ehp.7339

Oberdörster, G., Sharp, Z., Atudorei, V., Elder, A., Gelein, R., Kreyling, W., & Cox, C. (2004). Translocation of Inhaled Ultrafine Particles to the Brain. *Inhalation Toxicology*, *16*(6–7), 437–445. https://doi.org/10.1080/08958370490439597

Popovicheva, O., Engling, G., Lin, K. T., Persiantseva, N., Timofeev, M., Kireeva, E., Völk, P., Hubert, A., & Wachtmeister, G. (2015). Diesel/biofuel exhaust particles from modern internal combustion engines: Microstructure, composition, and hygroscopicity. *Fuel*, *157*, 232–239. https://doi.org/10.1016/J.FUEL.2015.04.073

Qian, Y., Qiu, Y., Zhang, Y., & Lu, X. (2017). Effects of different aromatics blended with diesel on combustion and emission characteristics with a common rail diesel engine. *Applied Thermal Engineering*, *125*, 1530–1538. https://doi.org/10.1016/j.applthermaleng.2017.07.145

Roedding, A. S., Gao, A. F., Wu, A. M. L., Li, P. P., Kish, S. J., & Warsh, J. J. (2009). TRPC3 protein is expressed across the lifespan in human prefrontal cortex and cerebellum. *Brain Research*, *1260*, 1–6. https://doi.org/10.1016/j.brainres.2008.12.069

Shi, L., Steenland, K., Li, H., Liu, P., Zhang, Y., Lyles, R. H., Requia, W. J., Ilango, S. D., Chang, H. H., Wingo, T., Weber, R. J., & Schwartz, J. (2021). A national cohort study (2000–2018) of long-term air pollution exposure and incident dementia in older adults in the United States. *Nature Communications*, *12*(1). https://doi.org/10.1038/S41467-021-27049-2

Shin, S., Burnett, R. T., Kwong, J. C., Hystad, P., Van Donkelaar, A., Brook, J. R., Copes, R., Tu, K., Goldberg, M. S., Villeneuve, P. J., Martin, R. V., Murray, B. J., Wilton, A. S., Kopp, A., & Chen, H. (2018). Effects of ambient air pollution on incident Parkinson's disease in Ontario, 2001 to 2013: A population-based cohort study. *International Journal of Epidemiology*, *47*(6), 2038–2048. https://doi.org/10.1093/IJE/DYY172

Strickland, J. D., Lefew, W. R., Crooks, J., Hall, D., Ortenzio, J. N. R., Dreher, K., & Shafer, T. J. (2015). In vitro screening of metal oxide nanoparticles for effects on neural function using cortical networks on microelectrode arrays. *Nanotoxicology*, *10*(5), 619–628. https://doi.org/10.3109/17435390.2015.1107142

Strickland, J. D., LeFew, W. R., Crooks, J., Hall, D., Ortenzio, J. N. R., Dreher, K., & Shafer, T. J. (2016). In vitro screening of silver nanoparticles and ionic silver using neural networks yields differential effects on spontaneous activity and pharmacological responses. *Toxicology*, *355–356*, 1–8. https://doi.org/10.1016/j.tox.2016.05.009

Tibuakuu, M., Michos, E. D., Navas-Acien, A., & Jones, M. R. (2018). Air Pollution and Cardiovascular Disease: a Focus on Vulnerable Populations Worldwide. *Current Epidemiology Reports*, *5*(4), 370–378. https://doi.org/10.1007/s40471-018-0166-8

Traboulsi, H., Guerrina, N., Iu, M., Maysinger, D., Ariya, P., & Baglole, C. (2017). Inhaled Pollutants: The Molecular Scene behind Respiratory and Systemic Diseases Associated with Ultrafine Particulate Matter. *International Journal of Molecular Sciences*, *18*(2), 243. https://doi.org/10.3390/ijms18020243

Tsai, J.-H., Chen, S.-J., Huang, K.-L., Lee, W.-J., Kuo, W.-C., & Lin, W.-Y. (2011). Characteristics of particulate emissions from a diesel generator fueled with varying blends of biodiesel and fossil diesel. *Journal of Environmental Science and Health, Part A*, *46*(2), 204–213. https://doi.org/10.1080/10934529.2011.532444

Tsolakis, A. (2006). Effects on Particle Size Distribution from the Diesel Engine Operating on RME-Biodiesel with EGR. *Energy and Fuels*, *20*(4), 1418–1424. https://doi.org/10.1021/EF050385C

Tukker, A. M., Wijnolts, F. M. J., de Groot, A., & Westerink, R. H. S. (2018). Human iPSC-derived neuronal models for in vitro neurotoxicity assessment. *NeuroToxicology*, *67*(November 2017), 215–225. https://doi.org/10.1016/j.neuro.2018.06.007

Valand, R., Magnusson, P., Dziendzikowska, K., Gajewska, M., Wilczak, J., Oczkowski, M., Kamola, D., Królikowski, T., Kruszewski, M., Lankoff, A., Mruk, R., Marcus Eide, D., Sapierzyński, R., Gromadzka-Ostrowska, J., Duale, N., Øvrevik, J., & Myhre, O. (2018). Gene expression changes in rat brain regions after 7- and 28 days inhalation exposure to exhaust emissions from 1st and 2nd generation biodiesel fuels - The FuelHealth project. *Inhalation Toxicology*, *30*(7–8), 299–312. https://doi.org/10.1080/08958378.2018.1520370

Vassallo, A., Chiappalone, M., De Camargos Lopes, R., Scelfo, B., Novellino, A., Defranchi, E., Palosaari, T., Weisschu, T., Ramirez, T., Martinoia, S., Johnstone, A. F. M., Mack, C. M., Landsiedel, R., Whelan, M., Bal-Price, A., & Shafer, T. J. (2017). A multi-laboratory evaluation of microelectrode array-based measurements of neural network activity for acute neurotoxicity testing. *NeuroToxicology*, *60*, 280–292. https://doi.org/10.1016/j.neuro.2016.03.019

Weichenthal, S., Olaniyan, T., Christidis, T., Lavigne, E., Hatzopoulou, M., Van Ryswyk, K., Tjepkema, M., & Burnett, R. (2020). Within-city Spatial Variations in Ambient Ultrafine Particle Concentrations and Incident Brain Tumors in Adults. *Epidemiology (Cambridge, Mass.)*, *31*(2), 177. https://doi.org/10.1097/EDE.0000000000001137

WHO. (2013). *Review of evidence on health aspects of air pollution–REVIHAAP Project*.

WHO. (2016). *Ambient air pollution: A global assessment of exposure and burden of disease*.

Xu, K., Yang, Z., Shi, R., Luo, C., & Zhang, Z. (2016). Expression of aryl hydrocarbon receptor in rat brain lesions following traumatic brain injury. *Diagnostic Pathology*, *11*(1). https://doi.org/10.1186/S13000-016-0522-2

Zerboni, A., Rossi, T., Bengalli, R., Catelani, T., Rizzi, C., Priola, M., Casadei, S., & Mantecca, P. (2022). Diesel exhaust particulate emissions and in vitro toxicity from Euro 3 and Euro 6 vehicles. *Environmental Pollution*, *297*, 118767. https://doi.org/10.1016/j.envpol.2021.118767

Zhang, L., Ru, B., Liu, Y., Li, M., Li, B., Wang, L., Xu, L., Le Guyader, L., & Chen, C. (2012). The dose-dependent toxicological effects and potential perturbation on the neurotransmitter secretion in brain following intranasal instillation of copper nanoparticles. *Http://Dx.Doi.Org.Proxy.Library.Uu.Nl/10.3109/17435390.2011.590906*, *6*(5), 562–575. https://doi.org/10.3109/17435390.2011.590906

Zhu, F., Ding, R., Lei, R., Cheng, H., Liu, J., Shen, C., Zhang, C., Xu, Y., Xiao, C., Li, X., Zhang, J., & Cao, J. (2019). The short-term effects of air pollution on respiratory diseases and lung cancer mortality in Hefei: A time-series analysis. *Respiratory Medicine*, *146*, 57–65. https://doi.org/10.1016/j.rmed.2018.11.019

Zielinska, B., Sagebiel, J., Mc Donald, J. D., Whitney, K., & Lawson, D. R. (2004). Emission rates and comparative chemical composition from selected in-use diesel and gasoline-fueled vehicles. *Journal of the Air and Waste Management Association*, *54*(9), 1138–1150. https://doi.org/10.1080/10473289.2004.10470973

Zwartsen, A., Hondebrink, L., & Westerink, R. H. (2018). Neurotoxicity screening of new psychoactive substances (NPS): Effects on neuronal activity in rat cortical cultures using microelectrode arrays (MEA). *NeuroToxicology*, *66*, 87–97. https://doi.org/10.1016/j.neuro.2018.03.007